In network processing for tectonic monitoring

Tran, Hoang Ha

2014

Tran, H. H. (2014). In network processing for tectonic monitoring. Doctoral thesis, Nanyang Technological University, Singapore.

https://hdl.handle.net/10356/61653

https://doi.org/10.32657/10356/61653

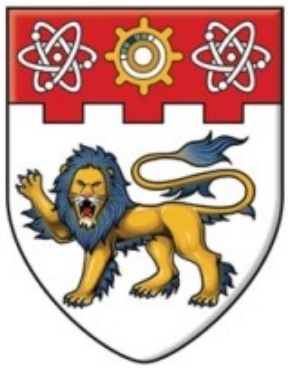

NANYANG TECHNOLOGICAL UNIVERSITY

IN NETWORK PROCESSING FOR TECTONIC MONITORING

TRAN HOANG HA

SCHOOL OF COMPUTER ENGINEERING

2014

IN NETWORK PROCESSING FOR

TECTONIC MONITORING

TRAN HOANG HA

School of Computer Engineering

A thesis submitted to the Nanyang Technological University
in partial fulfilment of the requirement for the degree of
Doctor of Philosophy

2014

ABSTRACT

The wireless mesh network connection between GPS stations empowers them with the ability to share information and adjustments with each other in real-time. The main focus of this research is to utilize wireless mesh network with three main directions 1) communication bandwidth reduction, 2) real-time event detection and 3) in-network GPS data processing.

Wireless mesh networking (WMN) is proposed to reduce the number of satellite links and bandwidth required for transmission of GPS data. WMN can be established using long range radios. Clusters of GPS stations will then be formed and a cluster-head is selected for each cluster. Each cluster-head will have satellite communication capabilities and will be responsible for collecting and compressing all the observation data from the GPS stations within the cluster and transmitting them to the remote centralized data server. This greatly reduces the number of satellite upload links needed when each cluster requires a minimum of only one satellite upload link. Furthermore, the cluster based GPS data compression could reduce 70% of daily upload data in our experiment.

In-situ parallel and distributed processing of GPS corrections can be made possible using mesh networking. The observation data from adjacent GPS stations are grouped together and processed in hierarchy fashion. Compared to conventional sequential processing method, the computational complexity and computation time of parallel and distributed GPS processing with various schemes decrease significantly. By sharing data within the mesh network, it is possible for in-network processing to be performed for GPS corrections using the embedded processing capability at each GPS station. This allows

early-warning applications to be developed without the need for costly data transmission to a remote centralized server. Moreover, event detection algorithm using single station may fail to identify events that are caused by noisy data or human made events. The collaboration GPS processing to have better detect seismic events could possibly be implemented by mesh network connections.

This thesis summarizes our work on the research topic of in network processing for tectonic monitoring. It investigates the use of mesh network connections between stations to able in-network processing.

ACKNOWLEDGEMENTS

This work could not have reached this state without the dedicated guidance and support from my supervisors, Prof. Wong Kai Juan and Prof. Lee Bu Sung. I am grateful to them for helping me during my four years of graduate student at Nanyang Technological University (NTU). Without their patience, understanding and encourage, I could not keep focus on my research direction and fully comprehend the research topic.

I would like to thank staffs and technicians in the Emerging Research Lab for their kindly assisted me in many aspects and provided me a friendly and convenient working environment.

I would like to thank all my friends, who helped me due with difficulty in my studying and daily life at NTU. I especially thank my mother, father and elder brother who provided unconditional love and care. Finally yet importantly, I would like to dedicate this dissertation work to my family especially my wife Linh and my daughter Mai for their understanding, encouragement and unconditional love.

TABLE OF CONTENTS

LIST OF FIGURES

LIST OF TABLES

CHAPTER 1

INTRODUCTION

1.1. Research Background

In recent years, volcanic eruptions and tectonic plate movements have caused big natural disasters, such as the Great Sumatra-Andaman earthquake [1-4] and the resulting Asian tsunami, which led to significant loss of human lives and properties. Scientific evidences [5, 6] proved it was the beginning of a new earthquake supper-cycles [5] in this active area. In order for scientists to further study such disasters and provide early warning of imminent seismic and volcanic events, many continuous-Global Positioning System (cGPS) arrays [7-15] were developed and deployed to monitor some of the active volcanic areas and tectonic plates around the world. Each of these cGPS array contains tens to hundreds of GPS stations; varying methods were used for collecting data from these stations. For the cGPS arrays were deployed in Andes [8] and Himalaya [9], GPS data was collected manually. In other deployments, such as GEONET [11] and SCIGN [12], telemetry was achieved from some stations using a modem connected to the telephone line. In other cGPS arrays for example the NZNSN [10] or Sumatran continuous-Global Positioning System Array (SuGAr) [7], due to the lack of wired telecommunication infrastructures, satellite communications were used as the primary means for telemetry. In other cGPS arrays were deployed in a small area such as Taal [13], Gunung Pa-

pandayan [14] or WiLSoN [15], due to the lack of wired and cellular telecommunication facilities, long-range line-of-sight (LoS) wireless communications were used to up-load data to a local processing facility before relay to a centralized server.

In cGPS arrays utilizing satellite or long-range LoS wireless communications, each GPS station in the cGPS array will periodically (usually from milliseconds to hours) measure the tectonic and/or meteorological data and store the data locally. This observed GPS data is sent to a data aggregation server through a dedicated uplink at various update intervals ranging from hours, days to months. At the server, the collected data from the GPS stations is processed with preprocessed correction information.

For cGPS array taking advantage of satellite communications, the communication bandwidth and the number of uplinks are the most important factors in terms of operational expenditure. Each satellite link requires costly subscription and data transmission across these links is usually charged based on the connection time or the amount of data transmitted/received. It could cost network operator hundreds of thousands to millions of dollar for satellite data subscription every year. Due to the high cost, operators could only afford to upload low sampling rate GPS data, bigger than two minutes sampling rate and employ daily to monthly data upload scheme. Therefore, in order to reduce the operational cost of a cGPS array, it is paramount that the number of satellite links as well as the data sent on these links is kept to a minimum.

For long-range GPS station using LoS wireless communications, the number of uplinks is the most important factors in terms of network construction expenditure. Each link requires well-constructed and carefully selected antenna mounting base to keep antennas in line; hence, in order to reduce the construction and maintenance cost of a cGPS array, the number of uplink and the amount of upload data are kept to a minimum.

1.2. Motivation

Post event processing method is the widely used technique to processing GPS data from remote cGPS arrays (e.g. Sumatran, Andes, Himalaya, Taal or Gunung Papandayan). These cGPS arrays located at far-off locations and some of the station located near hazardous and hard to access like active volcanic plates, which lack of wired telecommunication infrastructures. Hence, they have to make use of costly satellite subscription, long-range line-of-sight wireless connections or even manual data downloading method to send GPS data to centralized processing facility. As a result, it takes days to months to collect and process GPS data, which is inadequate for instantaneous responses in case of big tectonic or volcanic events occurred.

In order to reduce GPS data collection time, satellite subscriptions cost and make use of high frequency GPS data which could be stored locally at each GPS station; long range wireless mesh network is proposed and studied in this research. Wireless mesh network makes use of long-range multi-hop of point-to-point wireless connections between GPS stations to exchange GPS data and corrections that share between stations within network. Furthermore, it makes collaboration cluster based GPS processing possible to estimate stations' location within cGPSs network in near real-time. The aims of this research are:

- Decreasing number of costly communication subscription satellite up-links and/or power consumption long range radio uplinks of cGPS array which is studied in chapter 3,
- Reducing transmitted GPS data between stations in cGPS network and centralized processing facility which is studied in chapter 3,

- Utilizing high sampling rate GPS data at local station which costly to upload to centralized server in real-time which is studied in chapter 5,
- Paralleling GPS processing by make use of small, low and spare computation power within the GPS network which is studied in chapter 4.

1.3. Outline of The Thesis

This thesis consists of seven chapters.

Chapter 1 – *Introduction*. A brief summary of the background of this research is provided. The reasons motivating this research are summarized, outline of this thesis is presented and contributions of this research are highlighted.

Chapter 2 – *Literature survey*. A survey of GPS processing technique, GPS for tectonic monitoring, wireless sensor network for seismic monitoring, and GPS processing software are presented.

Chapter 3 – *Mesh networking for GPS data compression*. Mesh networks were created using multi-hop and long-range wireless communication between GPS stations and clusters are formed. A station in each cluster was selected to be the header of each cluster in order to process observed GPS data from all stations within the cluster.

Chapter 4 – *Parallelizing the computation of GPS processing*. The processing of GPS data in a parallel manner is studied and presented. The aim of this study is to reduce the computational complexity and decrease the number of arithmetic calculations required to estimate stations location.

Chapter 5 – *In-network single-frequency GPS processing*. In-network single-frequency GPS processing method is proposed. Four case studies of proposed processing

method using real single-frequency GPS data collected at Taal network are evaluated in this chapter.

Chapter 6 – *Proof of concept deployment*. The early results of an ongoing research of an in-network single-frequency GPS system is presented in this chapter.

Chapter 7 – *Summary and conclusions*. The final chapter of this thesis includes a brief summary of the research results, recommendations for future research.

1.4. Contributions

The contributions of this research could be summarized as follows:

- Wireless mesh network has been proposed and designed for seismic monitoring cGPS array by mean of long-range radios and data aggregation is performed to enable cluster-based compression. Using the actual data captured from the Sumatran cGPS array in the evaluation and analysis processing, the results show mesh networking not only reduces the number of costly satellite uplinks required, it also significantly reduces the total amount of data transferred through these links.
- GPS receivers in a GPS array are divided into groups with share common parameters and reference receivers. They will be processed in parallel, distributed and hierarchy fashion. This method significantly decreases the computational complexity and processing time. By reducing the computational complexity, the proposed computation model promises to make use of small, low and spare computation power within the GPS network.
- In-network distributed single-frequency GPS processing is studied. Various network setups are studied to evaluate the proposed method. The results show,

1) Location errors are very sensitive to communication channel errors especially when stations are more than two hops away from the cluster head, 2) The bandwidth required for daily solution is well supported by low power long-range radio module and 3) The proposed in-network single-frequency GPS method noticeably reduces the number of long-range uplink required for GPS network.

CHAPTER 2

LITERATURE SURVEY

In this chapter, Global Positioning System (GPS), GPS processing techniques, GPS network for tectonic monitoring, wireless sensor networks for seismic monitoring, and GPS processing software are briefly presented.

2.1. The Global Positioning System

The first global positioning system (GPS) satellite, which launched on 22 February 1978, and became fully operation on 27 April 1995, has opened up a new era of positioning. The GPS system is maintained and operated by the U.S. Department of Defense. The main purpose of this satellite system is to support the U.S. military and national security in specifying the position and time all over the world in any weather condition 24 hours a day. The constellation of this system nominally includes 24 out of 31 active satellites. Satellites orbit about 20,000 km above the Earth's surface, in six orbit planes. The planes are at 55 degrees with respect to the equator plane.

The navigation messages are transmitted with frequencies L1 at 10.23 x 154 = 1575.42 MHz (having wavelength $\lambda_1 \approx 19.0$cm) and L2 at 10.23 x 120 = 1227.6 MHz (having wavelength $\lambda_2 \approx 24.4$cm). They are modulated with two types of codes. The slower Coarse/Acquisition (C/A) code has a chipping rate of 1.023 MHz and it is meant

for civilian purposes. The Precision (P) code is ten times faster than the C/A code, and it is encrypted for military purposes. At present, the L1 carrier is modulated with both C/A and P codes, while L2 is modulated only with the P code. The more modern GPS transmits a second civilian-use code on L2 frequencies, L2C, and a third civilian code, first transmitted from the IIR(M)-20 satellite on 10 April 2009, is transmitted in a new carrier frequency L5 at 10.23 x 115 = 1176.45 MHz.

The GPS system provides two levels of service, the Standard Positioning Service (SPS) and the Precise Positioning Service (PPS). The civilian SPS, using L1 C/A-code positioning, is a positioning and timing service, which is available for all users without service charge. Until the discontinuation of selective availability (SA), SPS positioning accuracy was 100 m horizontally and 156 m vertically, and the time transfer accuracy was 340 ns (with 95% probability). The United States decided to discontinue use of SA at 4.00 UTC on 2 May 2000. As a result, the civilian C/A-code was immediately improved at 20 m. The PPS makes use of encrypted P code, which provides predictable positioning accuracy better than 22 m (95 %) horizontally, 27.7 m vertically and time accuracy to UTC within 200 ns (95 %) for U.S. Military use. The anti-spoofing capability of the P code prevents enemies mimicking the GPS signals by sending bogus information.

The International GPS Service (IGS) was established on 21 June 1992 and later renamed the International GNSS (Global Navigation Satellite Systems) Service in 2005 [16, 17]. It is a voluntary federation to archive and generate precise GPS/GLONASS products. IGS products [18] include GNSS observation data from the IGS network, GNSS orbits, Earth orientation parameters, satellite and clock information with different latencies and accuracies. IGS products are utilized to remove error sources, which affect

the accuracy of GNSS measurements due to the ephemeris/orbital, satellite clock, receiver clock, ionosphere, troposphere and multipath errors.

A brief overview of the pseudo-range measurement, carrier-phase measurement and different GPS processing methods are described in the following subsections.

2.1.1. Pseudo-range and carrier-phase measurement

Pseudo-range is associated with the distance between the satellite's antenna and the receiver's antenna. The code transmission is measured by correlating the pseudorandom noise (PRN) code generated by the satellites with the same code generated locally by the receivers. The code is generated by the satellites and the receivers are based on their own clock which leads to unpreventable timing errors.

The equation of a pseudo-range measurement in a vacuum space is shown in (2.1), where the subscript is the name of the receiver and superscript is the name of the satellite [19].

$$\rho_k^p(t) = (t_k - t^p)c = (t_k + dt_k - t^p - dt^p)c \tag{2.1}$$

in which:

$\rho_k^p(t)$: Geometric distance between the antenna of the satellite p and the antenna of the receiver k,

t_k : True time at the receiver's epoch k when the satellite code entered the antenna,

t^p : True time at the satellite p when the code is transmitted,

c: Velocity of light,

dt_k : Clock error at receiver k,

dt^p : Clock error at satellite p.

Therefore, the pseudo-range observation as a the function of the vacuum pseudo-range distance is

$$P_k^p(t) \equiv (t_k - t^p)c = \rho_k^p(t) - cdt_k + cdt^p \tag{2.2}$$

Moreover, the pseudo-range is affected by the ionosphere, troposphere, and delay errors at both satellites and receivers. Thus, the final pseudo-range function is

$$P_k^p(t) = (t_k - t^p)c = \rho_k^p(t) - cdt_k + cdt^p + I_{k,1,P}^p(t) + T_k^p(t) + \delta_{k,1,P}^p(t) + \varepsilon_{1,P} \tag{2.3}$$

$$\rho_k^p(t) = \left\| \mathrm{x}^p - \mathrm{x}_k \right\| = \sqrt{(x^p - x_k)^2 + (y^p - y_k)^2 + (z^p - z_k)^2} \tag{2.4}$$

$$\text{where, } \delta_{k,1,P}^p(t) = d_{k,1,p}(t) + d_{1,p}^p(t) + d_{k,1,p}^p(t) \tag{2.5}$$

$I_{k,1,P}^p(t)$: Ionospheric P-code delay of frequency L1 from satellite p to receiver k,

$T_k^p(t)$: Tropospheric delay – which depends on the troposphere along the propagation path not the frequency of the signal.

$\varepsilon_{1,P}$: Pseudo-range measurement noise of frequency L1 with P code,

$d_{k,1,p}(t)$: Receiver hardware delay,

$d_{1,p}^p(t)$: Satellite hardware delay,

$d_{k,1,p}^p(t)$: Multipath delay.

The phase measurement for the signals at frequency f_1 arriving at the receiver's antenna at time t is:

$$\varphi_{k,1}^p(t) = \frac{f_1}{c}\rho_k^p(t) + N_k^p(1) - f_1 dt_k + f_1 dt^p - I_{k,1,\varphi}^p(t) + \frac{f_1}{c}T_k^p(t) + \delta_{k,1,\varphi}^p(t) + \varepsilon \tag{2.6}$$

$$\delta^{p}_{k,1,\varphi}(t) = d_{k,1,\varphi}(t) + d^{p}_{1,\varphi}(t) + d^{p}_{k,1,\varphi}(t) \tag{2.7}$$

where the new parameters in Equation (2.6) are

$N^{p}_{k}(1)$: Integer ambiguity, with its value unchanged until a cycle slip happen,

$I^{p}_{k,1,\varphi}(t)$: Ionosphere delay for frequency L1,

$\delta^{p}_{k,1,\varphi}(t)$: Hardware delay and multipath of frequency L1,

$\varepsilon_{1,\varphi}$: L1 measurement noise

The carrier-phase can be scaled to unit length by multiplying by $\gamma = c/f$.

$$\phi^{p}_{k,1}(t) = \rho^{p}_{k}(t) + \lambda_1 N^{p}_{k}(1) - cdt_k + cdt^{p} - I^{p}_{k,1,\phi}(t) + T^{p}_{k}(t) + \delta^{p}_{k,1,\phi}(t) + \varepsilon_{1,\phi} \tag{2.8}$$

2.1.2. Differencing GPS measurement

To remove the common parameters between receivers, satellites and epochs, single-difference, double-difference and triple-difference are formed. The single-difference carrier-phase measurement between satellite p and two receivers, k and l, with a single-frequency L1 is derived as

$$\begin{aligned}\varphi^{p}_{kl,1}(t) = \frac{f_1}{c}\rho^{p}_{kl}(t) + N^{p}_{kl}(1) - f_1(dt_k + dt_l) - I^{p}_{kl,1,\varphi}(t) + \frac{f_1}{c}T^{p}_{kl}(t) \\ + d_{kl,1,\varphi}(t) + d^{p}_{kl,1,\varphi}(t) + \varepsilon^{p}_{kl,1,\varphi}\end{aligned} \tag{2.9}$$

In the above equation, the additional notation for single-difference of distance, integer ambiguity, ionosphere, troposphere, receiver hardware delay, multipath delay and measurement noise are

$$\rho^{p}_{kl}(t) = \rho^{p}_{k}(t) - \rho^{p}_{l}(t) \tag{2.10}$$

$$N_{kl}^{p}(1) = N_{k}^{p}(1) - N_{l}^{p}(1) \tag{2.11}$$

$$I_{kl,1,\varphi}^{p}(t) = I_{k,1,\varphi}^{p}(t) - I_{l,1,\varphi}^{p}(t) \tag{2.12}$$

$$T_{kl}^{p}(t) = T_{k}^{p}(t) - T_{l}^{p}(t) \tag{2.13}$$

$$d_{kl,1,\varphi}(t) = d_{k,1,\varphi}(t) - d_{l,1,\varphi}(t) \tag{2.14}$$

$$d_{kl,1,\varphi}^{p}(t) = d_{k,1,\varphi}^{p}(t) - d_{l,1,\varphi}^{p}(t) \tag{2.15}$$

$$\varepsilon_{kl,1,\varphi}^{p} = \varepsilon_{k,1,\varphi}^{p} - \varepsilon_{l,1,\varphi}^{p} \tag{2.16}$$

If two receivers, k and l, receive signals from the same two satellites, p and q, the double-difference phase observation could be derived as

$$\varphi_{kl,1}^{pq}(t) = \frac{f_1}{c}\rho_{kl}^{pq}(t) + N_{kl}^{pq}(1) + I_{kl,1,\varphi}^{pq}(t) + \frac{f_1}{c}T_{kl}^{pq}(t) + d_{kl,1,\varphi}^{pq}(t) + \varepsilon_{kl,1,\varphi}^{pq} \tag{2.17}$$

in which

$$\rho_{kl}^{pq}(t) = \rho_{kl}^{p}(t) - \rho_{kl}^{q}(t) \tag{2.18}$$

$$N_{kl}^{pq}(1) = N_{kl}^{p}(1) - N_{kl}^{q}(1) \tag{2.19}$$

$$I_{kl,1,\varphi}^{pq}(t) = I_{kl,1,\varphi}^{p}(t) - I_{kl,1,\varphi}^{q}(t) \tag{2.20}$$

$$T_{kl}^{pq}(t) = T_{kl}^{p}(t) - T_{kl}^{q}(t) \tag{2.21}$$

$$d_{kl,1,\varphi}^{pq}(t) = d_{kl,1,\varphi}^{p}(t) - d_{kl,1,\varphi}^{q}(t) \tag{2.22}$$

$$\varepsilon_{kl,1,\varphi}^{pq} = \varepsilon_{kl,1,\varphi}^{p} - \varepsilon_{l,1,\varphi}^{q} \tag{2.23}$$

The most important properties of double-difference are that the clock error and hardware delay of both receivers are eliminated. The multipath error of the two receivers cannot be removed because it depends on the surrounding geometry of each receiver.

Integer ambiguity is very important for sub-millimeter level GPS processing. To estimate the other parameters, the triple-difference form between two epochs of two receivers with the same two satellites is formed in (2.24).

$$\Delta\varphi_{kl,1}^{pq}(t_2,t_1)=\frac{f_1}{c}\Delta\rho_{kl}^{pq}(t_2,t_1)+\Delta I_{kl,1,\varphi}^{pq}(t_2,t_1)+\frac{f_1}{c}\Delta T_{kl}^{pq}(t_2,t_1) + \Delta d_{kl,1,\varphi}^{pq}(t_2,t_1)+\Delta\varepsilon_{kl,1,\varphi}^{pq} \tag{2.24}$$

The evaluated parameters will then be reinserted in equation (2.17) to estimate the integer ambiguities.

2.1.3. GPS data compression

In order to reduce the amount of transmitted data, compressed GPS formats and compression methods are studied. For the purpose of archives and exchanges of GPS data, the most commonly used GPS exchange format is the Receiver Independent Exchange (RINEX) format and the current Version is 3.0 [20]. It contains raw data collected by one GPS station. This format defines three file types for observation data, navigation message and meteorological data.

The RINEX file format contains much redundant information in its data record section. As correlation exists between consecutive epochs in observed data, a compressed RINEX format called the CRINEX format [21], based on the fact that observation information are related between consecutive epochs, is proposed by Hatanaka. The differential operation for text and numeric data in the record section is calculated. The multiple-order differences, calculated from the series of epochs of the original RINEX file, are then written to the CRINEX file. CRINEX reduces storage space and transmission bandwidth as only the difference between the current epochs and some previous epochs is stored. The compression rate of observation data in the CRINEX format combined with text compression is a reduction of about 38% in comparison with that of using text compression of RINEX format files. The correlation between observation data of related

or nearby GPS stations is utilized in Chapter 3 of this thesis to reduce communication overheads.

2.2. GPS Processing Methods

In this part, the most commonly use GPS processing methods are briefly presented with focus on real-time GPS processing methods.

2.2.1. Point positioning

The point positioning processing method is used to estimate four coordinates, comprising three coordinates for the receiver antenna x_k and one for receiver clock error dt_k, using pseudo-range measurements. The carrier-phase is used for smoothing the pseudo-range if it is available. The satellite coordinates are assumed to be known and are corrected by using broadcast ephemeris. The ionospheric and tropospheric delays are estimated by using predefined models; hardware and multipath delays are neglected.

In the point positioning processing method, the dilution of precision (GDOP) is often used to select a subset of satellites (≥ 4 satellites) from the visible satellites to minimize GDOP. The relationship between the pseudo-range difference (Δρ) and the position difference (Δx) [22] is as follows:

$$\begin{bmatrix} \Delta\rho_1 \\ \Delta\rho_2 \\ . \\ . \\ \Delta\rho_n \end{bmatrix} = \begin{bmatrix} e_{11}\ e_{12}\ e_{13}\ 1 \\ e_{21}\ e_{22}\ e_{23}\ 1 \\ . \\ . \\ e_{n1}\ e_{n2}\ e_{n3}\ 1 \end{bmatrix} \begin{bmatrix} \Delta x_1 \\ \Delta x_2 \\ \Delta x_3 \\ c\Delta t \end{bmatrix} + \begin{bmatrix} v_1 \\ v_2 \\ . \\ . \\ v_n \end{bmatrix} \tag{2.25}$$

The compact form of (2.25) is

$$z = Hx + v \tag{2.26}$$

The 4x4 matrix H is formed by direction cosines e_{i1} e_{i2} e_{i3} from the receiver to the i^{th} satellite, and v is the random noise. The error between the estimated receiver antenna location and the exact receiver position is

$$\delta x = (H^T H)^{-1} H^T \mathrm{v} \tag{2.27}$$

in which, $H^T H$ is the measurement matrix and the GDOP is defined as the trace of the inversion matrix of the measurement matrix (2.28).

$$GDOP = \sqrt{trace(H^T H)^{-1}} \tag{2.28}$$

It is proved that increasing the number of satellites will decrease GDOP, which leads to a more precise solution. Consequently, the number of satellites that can be seen by each receiver should be increased. However, due to the limitations of computational power and energy of embedded devices, many methods [22, 23] are proposed to reduce the computational complexity in computing GDOP. The use of a neural network (NN) based methods [23] sufficiently decreases the computation time and improve accuracy given enough training time for the Back-Propagation Neural Networks (BPNN) method or enough training data for Propagation Neural Network (PNN) or General Regression Neural Network (GRNN) method. However, this supervised learning requires costly and time-consuming training procedures. The learned model may not be useful if the processing data deviates too much from the training data set. Another method based on Newton's identities [22] reduces the computational complexity of the GDOP computation. It manages to marginally reduce the number of floating point operations (152 floating point compared to 163 of the conventional LU decomposition method).

The following brief describes the close form position solution which is proposed by Bancroft [24] to compute the receiver antenna location. Exact four satellites are used and assumed to be a subset of the satellites that provide minimum GDOP.

To shorten the equation, the Minkowski function for four spaces is used (2.29)

$$\langle a,b\rangle = a_1b_1 + a_2b_2 + a_3b_3 - a_4b_4 = a^T Mb, \text{ in which } M = \begin{bmatrix} {}_3I_3 & 0 \\ 0 & -1 \end{bmatrix} \tag{2.29}$$

The pseudo-range equation from four satellites is given as

$$P_k^i - cdt_k = \left\| \mathrm{x}^i - \mathrm{x}_k \right\|, \qquad 1 \le i \le 4 \tag{2.30}$$

Squaring both sides of (2.30) and using notations from (2.32) to (2.34) we have

$$BMu = \alpha + \lambda\tau \tag{2.31}$$

where

$$u = [\mathrm{x}_k \quad cdt_k]^T, \quad v = [\mathrm{x}^i \quad P_k^i]^T, \quad \lambda = \frac{1}{2} < u,u >, \quad \alpha^i = \frac{1}{2} < v,v > \tag{2.32}$$

$$\alpha = [\alpha^1 \ \alpha^2 \ \alpha^3 \ \alpha^4]^T, \qquad \tau = [1\ 1\ 1\ 1]^T \tag{2.33}$$

$$B = \begin{bmatrix} x^1 & y^1 & z^1 & P_k^1 \\ x^2 & y^2 & z^2 & P_k^2 \\ x^3 & y^3 & z^3 & P_k^3 \\ x^4 & y^4 & z^4 & P_k^4 \end{bmatrix} \tag{2.34}$$

The value of u in Equation (2.31) is

$$u = MB^{-1}(\alpha + \lambda\tau) \tag{2.35}$$

Hence, λ is a function of u (receiver antenna coordinators and clock error). By substituting (2.35) into (2.32) for the value of λ, we will obtain a function of λ which gives two solutions for x_k coordination. Only one of them is a valid solution based on the ellipsoidal high. An in-depth study of the special configuration of the pseudo-range with only

four satellites with an indicator ellipsoid [25] which determines Loci is used. In the first case, if a discriminant point is on the edge of the indicator ellipsoid, there is a unique solution. In the second case, if the discriminant is one point inside the indicator ellipsoid there are two solutions. Lastly, if the discriminant point is outside the indicator ellipsoid, then no solution is found.

2.2.2. Precise point positioning

The Precise Point Positioning (PPP) method [26, 27], instead of processing all receivers concurrently by using the conventional double-difference method, makes use of a small group of high frequency and precise receivers to estimate the satellite clocks and constellation orbit parameters. The remaining receivers can use pre-estimated parameters to estimate the position of their stations one at a time. As a result, the computational burden of each station using this method significantly reduces.

Dual–frequency GPS receivers utilize both carrier-phase and pseudo-range linear combination to remove the effects of ionospheric errors. Tropospheric refraction, other ambiguities and station position will be estimated from the measurements. Single-frequency PPP [28, 29] provides some promising results, however, it will not be considered in this study. Due to the lack of differential error removal, all the errors have to be taken into account, including errors related to satellites, stations and reference frames [27]. Satellite effects include phase wind-up and satellite antenna offsets. Site displacement effects are caused by solid Earth tides, polar tides, ocean loading and Earth rotation parameters (ERP) as well as the receiver's antenna phase center offset.

The ionospheric-free mathematical model for the pseudo-range (2.36) and phase observation (2.37) of PPP processing method derived from (2.3) and (2.8) respectively is as follows

$$P_{k,IF}^{p} = \beta_f P_{k,1}^{p} - \gamma_f P_{k,2}^{p} = \rho_k^{p} - cdt_k + T_k^{p} + \varepsilon_P \tag{2.36}$$

$$\begin{aligned}\varphi_{k,IF}^{p} &= \beta_f \varphi_{k,1}^{p} - \gamma_f \varphi_{k,2}^{p} = \frac{f_1}{c}\rho_k^{p} - f_1 dt_k + \frac{f_1}{c}T_k^{p} + \beta_f N_{k,1}^{p} - \gamma_f N_{k,2}^{p} + \delta_{\varphi,IF} + \varepsilon_{\varphi,I} \\ &= \frac{f_1}{c}\rho_k^{p} - f_1 dt_k + \frac{f_1}{c}T_k^{p} + R_{\varphi,IF} + \varepsilon_{\varphi,IF}\end{aligned} \tag{2.37}$$

in which tropospheric delay is modeled as a product of zenith path delay (ZPD) and the mapping function (M) [30]. The ZPD model comprises the predominantly well-behaved hydrostatic part (ZPD_h) [31] and the volatile wet part (ZPD_w) [32]. The tropospheric model is

$$T_k^{p} = M_h ZPD_h + M_w ZPD_w \tag{2.38}$$

The PPP method is able to provide sub-centimeter accuracy in static mode and sub-decimeter accuracy in the kinematic mode for both post-processing and real-time processing modes. However, it suffers from long convergence period in the time required for PPP to achieve the centimeter-level from a cold start, and the lack of support infrastructures, precise orbit and clock offset. A complete discussion on the current status of PPP is presented by Bisnath and Gao [33].

2.2.3. Real-time precision point positioning

Real-time PPP implies the ability to process GPS data using the PPP method with latency of around seconds at the user stations. It requires real-time orbit processing, which required a global network of GPS stations sending dual-frequency GPS data to a processing center in real-time, and the ability to provide adjustments to users in real-time. The dissemination of real-time PPP estimated correction products is mainly divided into satellite-based and Internet-based methods.

The Internet-based real-time PPP system was developed by the Jet Propulsion Laboratory (JPL) of the National Aeronautics and Space Administration (NASA) is de-

scribed by Muellerschoen, et al. [34]. The system is called Internet-based Global Differential GPS (IGDG). It is able to deliver decimeter-level position accuracy to end users uniformly on the Earth. This system provides broadcast orbit and clock corrections for users via a TCP servers in real-time. The tests [34-36] show the standard deviation for positioning, both in static and kinematic modes, with dual-frequency users, provided an accuracy is about 10 cm in the horizontal component and 20 cm in the vertical component using both L1 and L2 frequencies.

Another implementation of real-time PPP is the StarFire system [37], a satellite-based system which transmits corrections using Inmarsat L-band communication frequencies (1525-1565 MHz). The receiver is equipped with only a single multifunction antenna to receive both L1 and L2 GPS frequencies and the Inmarsat signals. Users apply global wide area differential GPS or global real-time GPS corrections together with their ionospheric-free carrier-phase observations to estimate their positions. The epoch position solution at one-sigma accuracy horizontal is less than 10 cm.

In the methods mentioned above, users will receive the correction with some latency. It takes about 2 seconds to obtain the data set from the Internet and half a second to process the clock solution in the Internet-base real-time PPP method. For method using Inmarsat satellite, the uplink and downlink take 1.5 seconds each. For real-time applications due to the delay, the correction must be extrapolated over 4–5 seconds and this does not considerably decrease in the station's location accuracy [19].

Major research efforts are currently placed on enhancing the quality of high-rate real-time orbit and clock products [38, 39]. In particular, IGS has been studying real-time data products with the IGS real-time pilot project was started in 2007.

2.2.4. Relative positioning

Differential positioning GPS (DGPS) is a technique using more than two receivers to estimate the location of all or part of those receivers. Typically, one receiver is fixed with a known coordinate and the coordinates of other stations are estimated relate to the fixed station. With this method, double-difference or triple-difference observations are often used, even though single-difference observation could still be used.

The DGPS processing method is divided into two modes: post-processing mode and real-time mode. In post-processing mode, GPS observations within each processing interval are collected from stations and processed offline without any real-time communication among stations. The real-time DGPS processing mode is more complicated. It requires real-time or near real-time communication between reference stations and/or between reference stations and mobile stations. The observations or corrections from a single reference station or network of reference stations are broadcast to the roving users. Differential GPS techniques are classified according to

- Type of GPS measurement (pseudo-range or carrier-phase),
- Post-processed or real-time mode,
- Static or kinematic processing mode.

In-depth discussions about DGPS can be found in [19, 40]. The focus of this study is real-time GPS processing. As a result, only real-time positioning is presented in the following section.

2.2.5. Real-time relative positioning

In real-time relative positioning, calibrations in terms of pseudo-range and/or carrier-phase observation adjustments from the reference stations are sent to moving receivers

enabling them to compute their locations in real-time. Distributed on site GPS processing provides a real-time processing mechanism for kinematic applications to obtain precise relative locations with respect to some fixed stations. There are many methods of transmitting calibration data to users including via mobile phone networks, ground transmitters, satellites and the Internet. Based on the network coverage, real-time service could be categorized as follows:

- Local area differential GPS (LADGPS): This method uses a single reference station or a network of reference stations to evaluate pseudo-range or carrier-phase corrections. The corrections are broadcast by using ground-based beacon transmitters employing the Radio Technical Commission for Maritime Service (RTCM) [41] format. Beacons typically have a maximum broadcasting range of 100 km to 200 km. Typically this technique is used in kinematic mode and is known as Real-Time Kinematic (RTK). With a single reference station, the accuracy achieved is in the range of 1 m to 10 m. The enhancement of this method using a network of reference stations (network-RTK) [42] could achieve centimeter level accuracy.
- Wide Area Differential GPS (WADGPS): This method uses a network of reference stations, which includes at least one master station and a number of monitor reference stations to derive vectors of error corrections for each satellite. The accuracy of this method is nearly constant within the coverage region (hundreds to thousands kilometers). The evaluated error correction can be transmitted to users' receivers by any means communication, such as satellite, telephone or radio. It supports real-time accuracy for pseudo-range measurement in the range of decimeters to meters.

The estimated corrections are transmitted to users to reduce the telemetry budget and computation complexity of end-user receivers. Carrier-phase and pseudo-range calibration using one reference station are evaluated in the subsequent part of this section. The carrier-phase correction at epoch t sending from reference station k to station m [19] is

$$\Delta\phi_k^p = \rho_k^p - (\phi_{k,b}^p + \lambda K_k^p) - \mu_k \tag{2.39}$$

in which k is the integer correction and μ_k is the mean discrepancy of all satellites observed at epoch t. The carrier-phase correction is added to the rover's carrier-phase at station m for error calibration.

$$\bar{\phi}_m^p = \phi_m^p + \Delta\phi_k^p \tag{2.40}$$

The double-difference between the carrier-phase at the mobile station m with respect to two satellite p and q with correction received from station k is

$$\bar{\phi}_m^{qp} = \rho_m^{qp} + \lambda(N_{km}^{pq} + K_{km}^{pq}) + I_{km,\phi}^{pq} + T_{km}^{pq} + d_{km,\phi}^{pq} \tag{2.41}$$

The location of station m can be estimated by using the conventional double difference method with a modified ambiguity $N_{km}^{pq} + K_{km}^{pq}$ instead of N_{km}^{pq} as normal double difference method. The telemetry load can be reduced by decreasing the frequency of correction transmission and by sending the correction rate. The carrier-phase correction can be calculated by using the correction received at time t_0 and the correction rate:

$$\Delta\phi_k^p = \Delta\phi_k^p(t_0) + \frac{\partial\Delta\phi_k^p}{\partial t}(t - t_0) \tag{2.42}$$

The pseudo-range correction is calculated by using the same method for the carrier-phase as follows.

$$\Delta P_k^p = \rho_k^p - P_{k,b}^p - \mu_k \tag{2.43}$$

$$\overline{P}_m^p = P_m^p + \Delta P_k^p \tag{2.44}$$

$$\overline{P}_m^{qp} = \rho_m^{qp} + I_{km,P}^{pq} + T_{km}^{pq} + d_{km,P}^{pq} \tag{2.45}$$

In a network of multi reference stations, two requirements are necessary to calculate the mobile station's corrections; the centimeter level location of the reference station and the single-difference or double-difference integer ambiguity for the baseline between the references are known. The evaluated ionospheric and tropospheric corrections are broadcast by means of network coefficients over time. The mobile station interpolates the correction which is based on the estimated location. To reduce the computational complexity of the software at the mobile station without changing it, the virtual reference stations (VRS) is proposed [43]. In this method, the master reference station computes the correction based on the provided estimated location of the mobile stations. As the baselines between the virtual reference station and the mobile stations are very short (in the range of meters), either tropospheric or ionospheric corrections are not required at the mobile stations. Implementation of some of real-time relative positioning is described in the following paragraphs.

The first system NetAdjust [44, 45], which uses the network-RTK method to evaluate a set of corrections, will minimize the error variance between reference stations measurements and measurements of mobile receivers. First, the linear independent double-difference among networks of reference stations is calculated. Then, the differential code and phase errors within the region covered by the reference stations are evaluated using linear least-square predictors and least-square collocations. The prediction equations are evaluated for the un-differenced carrier-phase between each satellite at the reference stations and a grid of known locations. Finally, the mobile stations will use the

received predict covariance to calculate their locations. The real-time field test [42], at Tokyo in August/September 2000 using both dual-frequency receivers at the reference stations and mobile stations, gave a correction accuracy of 25 cm and 5 cm at the users' receivers located 70 km and 30 km respectively from the center of the reference network. At Calgary in September 2000, the corrections reached 5cm at a station 8km from the center with a data rate of 3 to 4 kps using the NovAtel binary format.

The real-time wide area differential GPS (WADGPS) system [46], is implemented by SALOC, is based on the RT-GIPSY software package. The system consists of 14 codeless dual-frequency geodetic receivers returning real-time data at a rate of 1 Hz. The system provides real-time ionospheric corrections with a vertical root mean square accuracy of 20 cm.

Another WADGPS proposed by the NavCom Technology [37] uses dedicated processing centers to evaluate the correction in real-time and uses geostationary communication satellites to broadcast the correction information for each satellite. The orbit corrections of each satellite are generated and transmitted every five minutes and clock corrections for each satellite are generated and transmitted every two seconds. The horizontal correction accuracy exceeds 10 cm.

2.3. GPS Processing Software

GPS processing software used in this research is briefly presented in this section.

2.3.1. Bernese GPS software

Bernese GPS software [47] is a commercial GPS post-processing package developed by the University of Bern. GPS and the Russian Global Navigation Satellite System (GLONASS) measurements are supported by Bernese GPS. The current version of the

Bernese GPS software is Version 5.0 released in April 2004. Its graphical user interface is based on the QT-library, which provides identical interfaces on the UNIX/Linux and Windows platforms. It supports the processing of a large number of receivers, which could be a combination of data from GPS, GLONASS, and GPS/GLONASS receivers. Both DD and PPP processing methods with mixed static and kinematic stations are supported by this software package. It can resolve ambiguity with long baselines up to 2000 km.

2.3.2. GAMIT/GLOBK/TRACK

GAMIT/GLOBK/TRACK [48] is a comprehensive GPS analysis package developed at MIT, the Harvard-Smithsonian Center for Astrophysics (CfA), and the Scripps Institution of Oceanography (SIO) for estimating station coordinates and velocities, stochastic or functional representations of post-seismic deformation, atmospheric delays, satellite orbits, and Earth orientation parameters. To control processing, it uses C-shell scripts, which run FORTRAN or C codes. The software is designed to run under any UNIX operating system supporting X-Windows. This program supports static (GAMIT package) and kinematic (TRACK package) DD processing modes.

2.3.3. GIPSY-OASIS

GIPSY-OASIS (GOA II) [49] is a combination of two earlier versions of GIPSY (GPS Interred Positioning System) and OASIS (Orbit Analysis and Simulation Software). It is a sophisticated software packages for general satellite tracking and orbit determination, which includes many special features, tailored for GPS applications. JPL developed GOA II with NASA funding. The processing capabilities include multi-station, multi-satellite and satellite-satellite processing models. GOA II is used to deter-

mine the position and velocity of fixed-location sites on the ground, or of moving vehicles on the land, in the sea, the air and space.

2.3.4. GPSTk

GPS Toolkit (GPSTk) [50] is an open source GPS processing library developed at the Applied Research Laboratories, The University of Texas, Austin. The source code is written in ANSI C++ and released under LGPL license. GPSTk supports standard input files such as RINEX Version 2.1, precise ephemeris processing (SP3), and low level Binary Exchange Format (BINEX). The positioning applications developed with GPSTk comprise standard pseudo-range-based positioning, differential phase-based positioning and PPP [51]. The PPP processing results of GPSTk are consistently within 10 cm from the IGS nominal value [51], which is considerably favorable compared to other commercial processing software. This library only supports short baselines for double-difference processing and requires fixed reference stations. It is free, small and portable providing a good GPS processing solution for embedded devices.

2.4. GPS Network for Tectonic and Volcanic Monitoring

GPS has become an interesting geodesy measurement method for studying a wide range of geophysical phenomena. GPS is used to monitor the Earth's tectonic plate motion, to study the deformation process around active faults, volcano deformation, glacial adjustment and sea-level studies. GPS is even able to provide atmospheric information by measuring the delays when GPS signals pass through the Earth's atmosphere (ionosphere and troposphere). GPS provides highly precise three-dimensional measurements accurate to a few millimeters to approximately one centimeter over long baselines ranging from hundreds of meters to thousands of kilometers. Three-dimensional measure-

ments emerging from GPS data allows the estimation of vertical and horizontal displacements at the same time and place, which other methods cannot provide.

The growth in crustal deformation research using GPS is mainly due to its light weight, precision and inexpensive properties compared to other space geodetic techniques, such as Very Long Baseline Interferometry (VLBI) and Satellite Laser Ranging (SLR) that require large facilities and substantial budgets. Consequently, small teams with lower budgets can utilize GPS for their studies. Furthermore, GPS could complement Interferometric Synthetic Aperture Radar (InSAR) by providing long-term measurements, deformation vectors and superior temporal coverage as compared to the wide spatial coverage of InSAR [52]. Moreover, GPS can also be used to provide atmospheric water vapor correction for InSAR measurements [53].

2.4.1. GPS Network for Tectonic Monitoring

GPS applications in earthquake studies [54] include co-seismic deformation, post-seismic and inter-seismic processes, often complementing seismological data. Post-seismic (except aftershocks) and inter-seismic deformations are much smaller than co-seismic measurements. Thus, there is little or no supporting information from seismic measurements. In this case, GPS measurements become the best method to detect long time interseismic strain accumulation which leads to identification of future earthquakes' location [52].

In order for scientists to study earthquakes and tsunamis and provide early warnings of imminent seismic events, many continuous-Global Positioning System (cGPS) arrays [7-12] are developed and deployed to monitor some of the active tectonic plates around the world. Each of these cGPS arrays contains tens to hundreds of GPS stations, spanning from hundreds to thousands of kilometers and varying methods are used for

collecting data from these stations. In the following paragraphs, some of these arrays are described.

The GPS Observation Network system (GEONET) deployed across Japan [55], comprising over 1200 GPS stations nationwide deployed, is one of the most dense cGPS networks, Figure 2-1. It is used to support real-time crustal deformation monitoring and location-based services. GEONET provides real-time 1 Hz data through a dedicated IP-VPN (Internet Protocol Virtual Private Network).

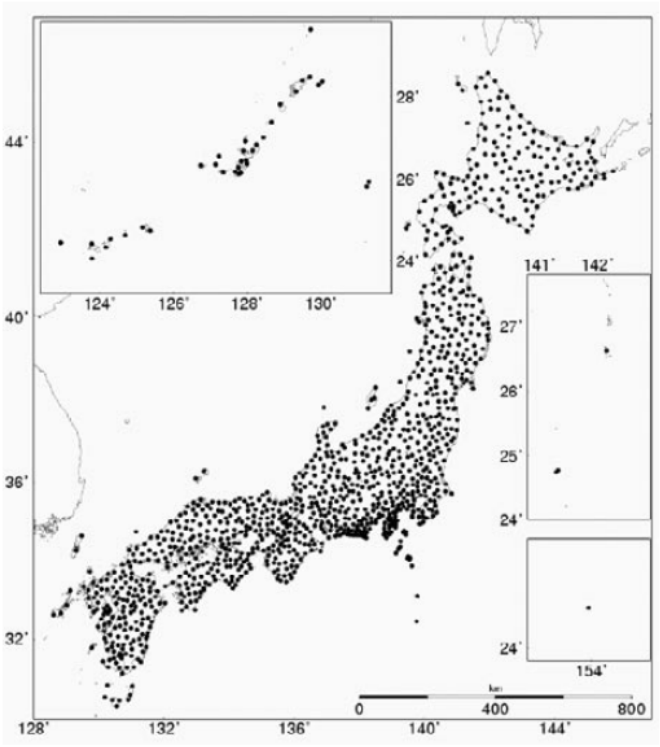

(*Atsushi Yamagiwa, et al.,, 2006* [55])

Figure 2-1 Geographical distributions of GEONET stations

The Southern California Integrated GPS Network (SCIGN) [12] contains more than 250 stations covering most of southern California which provides near real-time GPS data. It is collaboration between USGS, SOPAC and JPL. SCIGN is used to monitor fault interaction and post-seismic deformation in the eastern California shear zone.

The New Zealand GeoNet [10] is a nationwide network of broadband and strong ground motion seismometers, complemented by regional short period seismometers and cGPS stations, volcano-chemical analyzers, and remote monitoring capabilities. It comprises more than 150 cGPS stations spanning through New Zealand. All seismic and GPS data are transmitted continuously to two data centers using radio, land-based communication infrastructures and VSAT systems employing the Internet Protocol data transfer techniques.

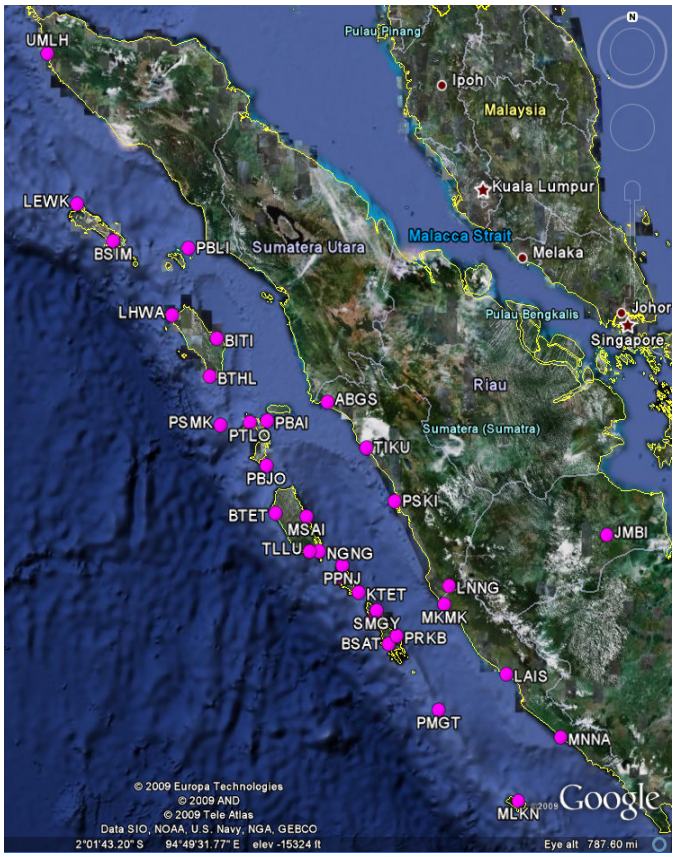

Figure 2-2 Geographical distributions of SuGAr stations

The Sumatran continuous-Global Positioning System Array (SuGAr) [7, 56] is located along Sumatra plate, Indonesia. At the end of 2009, it consisted of 32 operational GPS stations spanning 1400 km from the north to the south of Sumatra island (Figure 2-2). Stations are located in either remote islands or rural areas near the tectonic plate

boundary, one of the most active plates in the world. Due to the lack of a robust communication network infrastructure satellite telemetry is the only means of communication used by the GPS stations. All of the stations are equipped with a scientific grade GPS receiver, a GPS antenna, a satellite modem, solar panels, and batteries. SuGAr's GPS data is used in a study in Chapter 4 of this thesis.

2.4.2. GPS Network for Volcanic Monitoring

Early research on using a networks of single-frequency GPS systems for volcano deformation monitoring was conducted by the University NAVSTAR Consortium (UNAVCO) [57]. In this research, single-frequency carrier-phase and pseudo-range measurements are continuously transmitted to a central computing facility through TDMA radio. Epochs of GPS data are sent in pre-defined time slots and processed at hourly or shorter intervals with the intention to providing estimated station locations in near real-time. Each station consists of a GPS antenna, an RF antenna, a solar panel and a stainless steel casing box. The contents of the steel box include a CMC GPS receiver housed together with a FreeWave radio modem and a battery. The first NAVCO single-frequency GPS system was tested at Long Valley Caldera, California in 1998 and since then, it has been deployed on several volcanoes including Kilauea/Mauna Loa volcano Hawaii [58] and Taal volcano Philippines [13]. The data of the Taal single-frequency GPS array is used in Chapter 5 of this thesis.

The University of New South Wales (UNSW) has developed a prototype of a low-cost single-frequency system [59-61] installed on Mt. Papamdayan, Indonesia. The network consists of one base station located at the foot of the volcano and three slave stations located 8 km away around the crater of the volcano. Each station comprises five components: GPS module, radio modem, monument, GPS antenna, and power supply.

Data is collected at 15 s sampling rate. An hourly file is created and stored in the RAM of the slave station. The base station will send a command to collect hourly data from the slave stations every hour. Raw GPS data is converted to RINEX and stored on a hard disk at the base facility. Spare dual-frequency GPS stations surrounding the deformation zone of the volcano are used to generate ionospheric bias correction, which is applied to the localized single-frequency data processing. Such a mixed-mode GPS processing methods have shown their potential to achieve centimeter-level accuracy for epoch-by-epoch solutions.

The University of Applied Sciences of Southern Switzerland and GEODEV[62] have developed a commercially available single-frequency GPS system for geotechnical and civil engineering uses, namely the Movement Monitoring System. In this system, a network of single-frequency GPS stations is connected to a control unit via a cable, a GSM modem or a radio link. Maximum distance between stations is less than 20 km and the measurement frequency is less than two measurements per hour. GPS data is transmitted to the base station where the data is processed and archived. The baseline results can be used to automatically initiate warning or alarm messages via email or SMS if they exceed a certain pre-set limit. Even though this system is designed for structural monitoring, it could be utilized for volcano deformation monitoring.

The Real-Time Network processing Engine (RTNet) developed by GPS Solution Inc. is used to estimate ionospheric correction for the L1 GPS receiver network, utilizing real-time data collected from a dual-frequency GPS network, GEONET [63]. The system includes a Real-time Epoch Server (RTES) to collect and to store real-time dual-frequency GPS data. The RTNet server is used to estimate the ambiguity and ionospheric

delay. The system could process single-frequency GPS data in both kinematic and static modes with a tested base line from 9.2 km to 39 km.

In the above single-frequency GPS systems, a centralized server is always required to archive raw GPS data and to estimate station locations. Ionospheric bias correction is estimated at the server using the dual-frequency GPS data of the reference stations available in the network. Estimated bias is utilized to reduce the ionospheric effect when estimating single-frequency low-cost GPS station locations. This bias could be used at the centralized server in mixed-mode GPS processing method [61] or sent to another server to estimate the station locations in an RTNet system [63]. Since all the processing is performed at the server-side, the processing capability of each station/node in the network is not utilized to process GPS data. Furthermore, high frequency GPS data will have to be sent to a centralized server, which consumes much of the communication bandwidth and energy, and in some instances, increases the total operational cost to maintain the whole GPS network.

2.5. Wireless Mesh Network

Wireless mesh network is used in this thesis to enable in-network GPS processing. In this section the basic concept of wireless mesh network and the advantages of WMN over traditional networks is presented. The in-depth study about wireless mesh network could be found in [64] and [65].

2.5.1. Introduction

Wireless mesh network (WMN) is a multi-hop peer-to-peer wireless network, which nodes are connected in mesh topology. Nodes in this network comprise mesh routers, mesh clients, and gateways. Each node in the network could operate as a host

and/or as a router to forward packets send by others node in the network to their destinations. A WMN is dynamically self-organized and self-configured their connection in which the nodes automatically establishing and maintaining mesh connectivity among themselves.

2.5.2. Advantages of WMN

Reliability: each node in WMN acts as a relay to send packets to their destination. Due to the dynamic natural of network, nodes can enter and leave the mesh network, each node must have a capability to dynamic changing its forwarding pattern based upon its neighborhood. Consequently, the mesh topology enhances reliability of the network because the failure of one link and/or node will result in packets being forwarded via an alternative node toward their destination.

Self-Configuration: every node in a WMN store and discover their neighbor nodes and routing information to other nodes in the network. Therefore, nodes could be self-configuration without the intervention of network administration.

Self-Healing: nodes dynamically discover their neighbor nodes and routing information to other nodes in a WMN. As the result, nodes will automatic adjust to the failure or removal of a node by changing their communication paths, which results in a self-healing capability of WMN.

Scalability: the self-configuration and self-healing capability of WMN help to scale the network by just simply deploy or place new nodes in the communication range of the existing nodes.

2.6. Wireless Sensor Network for Seismic Monitoring

2.6.1. Introduction

Wireless sensor networks (WSN) for monitoring applications can be divided into two categories. The first group includes those applications which study the behavior of the systems required low sampling rates and low power consumption, such as networks deployed in Great Duck Island [66] and Redwood forest [67]. The second group includes those used to identify events in a system, requiring a high sampling rate and highly synchronized data. Health monitoring of machines [68], water supply monitoring [69], structural health monitoring [70], volcanic monitoring [71-73] and tectonic monitoring [15, 74] are applications in this group. This review focuses on the volcanic and tectonic monitoring WSN, which are deployed to monitor seismic events with long range and line-of-sight communication.

2.6.2. Seismology wireless sensor network

In the first example of this review, a WSN is used to monitor Volcán Tungurahua [71], an active volcano in central Ecuador. The network consists of three wireless nodes equipped with low-frequency acoustic sensors to collect infrasonic signals at 102 Hz, a data aggregator node located at the center of the network and a GPS receiver for time synchronization. Sensing nodes are placed 1 m to 10.7 m away from the aggregator node. Collected data is sent to a laptop base station 9 km away using FreeWave long-range wireless communication. Over 1.7 GB of uncompressed log data is collected over 54 hours of continuous data aggregation, including at least nine large explosions. The results show the correlation with the nearby wire infrasound node and the wire seismic sensor, thus proving the feasibility of using WSN to monitor an active volcano. However, the deployment lacks a data compression mechanism, power management, event-based data

logging triggers and only demonstrates quite narrow coverage areas as well as a small number of sensing nodes.

Another example of a mesh network for volcanic monitoring is the volcano network at Volcán Reventador [72, 73], an active volcano in northern Ecuador. The study was conducted with the data yield of 68.5% in 19 days. It consisted of 16 wireless sensor nodes continuously sampling seismic and acoustic data at 100 Hz with a Gamin GPS receiver for time synchronization. The WSN is formed between nodes spanning over 3 km with the distance between nodes ranging from 200 m to 400 m. Data is relayed to a gateway node by a multi-hops protocol and transmitted to the laptop base station via a long-range radio modem. Due to the multiple hop transmission and the lack of redundancy, a single node failure may pose a serious problem to the network. A triggering event collection mechanism with time-limited events is used to aggregate data from the sensing nodes. The laptop-station starts collecting data from the entire network when it receives enough event reports in a predefine time window. After an event is trigged, each node in the network pauses in the sampling and reporting events until it has uploaded all of its data. This collection method prevents a false event detected locally from triggering data collection of the whole network. However, it causes events to be undetected when a node is uploading its data or when the node pauses in its sampling process.

The wireless linked seismological network (WiLSoN) [15], a tectonic monitoring mesh network, is designed to transfer 24-bit, 100-sample/s data across 25 hops to the base station. WiLSoN covers half of the Middle American Subduction Experiment, which contains 100 sites. It runs nearly perpendicular to the Middle American trench through Mexico spanning 250 km. WiLSoN contains 50 seismic sites (the green sites in Figure 2-3) equipped with an 802.11b radio using 2.4 GHz frequency and line-of-sight

communication [75]. The distance between sites is from 5 km up to 43 km, deployed in a zigzag manner across the seismic array with extra repeaters used to overcome obstructions. The system collects about 2.5 GB of data daily and the data yield over the eight months experiment from the wireless sites is 78% compared to 86% at the stand-alone sites. The deployment shows the potential of WSN for rapid and dense sensing systems for active seismic monitoring. However, several challenges remain in increasing the yield, reliability, and time synchronization of the harvested data.

The next deployment of WiLSoN is for the Subduction Zone Seismic Experiment in Peru [74]. It includes 50 sites (Figure 2-4) which are wirelessly connected to each other with distances of 6 km among them. The 802.11b network is connected to the Internet at various sinks along the mesh network.

Adapted from [15]

Figure 2-3 Map of the 50 wireless UCLA sites in Mexico

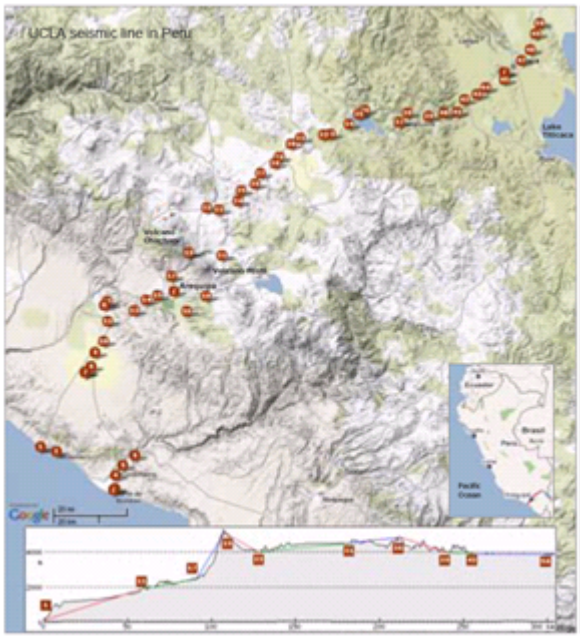

Adapter from [74]

Figure 2-4 Map of the 50 wireless UCLA sites in Peru

CHAPTER 3

MESH NETWORKING FOR GPS DATA COMPRESSION

In the previous chapter, the properties of Sumatra GPS array (SuGAr) and the challenges are described. In this chapter, modifications are proposed to utilize the mesh network in order to reduce the operation expenditure of satellite communication subscription of SuGAr array by removing correlation observation information and compressing observation GPS data. Part of the presented results in this chapter are published in Tran and Wong, "Mesh Networking for Seismic Monitoring - The Sumatran cGPS Array Case Study," WCNC 2009[76].

3.1. Proposed Modification for SuGAr

3.1.1. Removal of correlation information

The aim of the first modification is the removal of correlation information in the observation data at each GPS station. Observation data is measured at consecutive intervals, thus, correlation inherently exists between these consecutive measures (epochs). Therefore, instead of using the RINEX[77] file format, the CRINEX[78] (Compact RINEX) file format which utilizes the inherent correlation between consecutive epochs is used locally at

each GPS station to remove the correlation in the observation data. This step significantly reduces the size of the observation data and transmission overheads.

3.1.2. Mesh networking and cluster formation

Mesh network topology is an optimal topology to provide redundant connections between GPS stations than other network topologies like ring, bus, star or tree topology buy not as expensive to construct as full connected network topology. The redundancy connections are very critical when some of the connections could be lost during tectonic or seismic event occurred. The aim of mesh networking and clustering is to reduce the number of satellite links required. Wireless mesh networks can be established using long range radios such as those developed by FreeWare[79]. These radios provide a point-to-point line-of-sight (LoS) wireless communication link with a maximum range of more than 96 kilometers (60 miles) and a maximum over-the-air throughput of 154 Kbps. For communication links over a longer distance, multi-hop communications can be utilized by deploying relay stations. The use of relay stations may also overcome LoS obstructions between GPS stations as well as provide for extended mesh networking capabilities such as redundancy. Depending on the budget, geographical, power restriction or latency considerations, the number of hops and the radio range supported may be limited. In this case, clusters of GPS stations will be formed and a cluster-head would be selected for each cluster. Each cluster-head will have satellite communication capabilities and will be responsible for collecting all the observation data from the GPS stations within the cluster and transmitting them to the remote centralized data server. This greatly reduces the number of satellite links needed by the GPS network, as each cluster requires a minimum of only one satellite link.

3.1.3. Cluster-based compression at the cluster-heads

Each cluster-head will compress the observation data from all GPS stations within the cluster using the LZMA[80] algorithm prior to transmit via the satellite link. By default the LZMA algorithm uses 94 MB of RAM for compress and 9 MB of RAM for decompress, which could be fulfilling by most of the embedded system. Moreover, maximum memory usage for compression and decompress could be adjusted to meet memory constraint requirement of embedded system. The average compression time of LZMA algorithm run by an embedded system equipped with an ARM1176JZF-S run at 700 MHz and 512 MB RAM for daily, hourly and 2 minutely upload rate are shown in Table 3-1. The running time of the algorithm is met with the running speed constraints of the three data upload schemes.

	Daily	Hourly	2Minutely
Single station	20.266s	0.544s	0.103s
Cluster with all station	142.525s	3.586s	0.598s

Table 3-1 LZMA algorithm compression time

Compared to the existing SuGAr deployment where each GPS station transmits the observation data independently, the use of mesh networking allows larger datasets to be formed through the aggregation of observation data from each GPS station within a cluster. Given that the compression ratio increases in proportion to the size of the dataset to be compressed, the number of bytes transmitted via the satellite will be significantly reduced.

3.2. Empirical Study

To analyze the optimization achieved by the use of mesh networking on the SuGAr network, performance evaluation is studied using the archived SuGAr observation data for two months (61 days) of year 2007. Only 24 stations are taken into account in this case study as only they were able to provide the complete GPS dataset for the entire period. This experiment dataset can be accessed from the SOPAC website[81].

The assumptions made for the evaluations presented in this study are as follows

- All GPS stations have enough energy to deal with overheads caused by the additional communication equipment and the data computation required. This assumption can be satisfied by adding more batteries and solar panels to the existing nodes.
- To simplify the analysis, the terrain information between the GPS stations is not taken into consideration. In practice, construction of tall antenna towers as well as the use of multi-hop relays/repeaters can be used to overcome obstructions if required.
- The transmission overheads for the long range radios, such as packet formatting and control protocols, are not included in the evaluation as they will not have an impact on the analysis presented in this study.

The two main performance attributes of interest in this study are the reduction of the number of satellite links as well as the total amount of data transmitted via these links.

3.2.1. Uplinks reduction

Instead of communicating using dedicated satellite modem, each GPS station can also be equipped with one or more long-range radios such as the FreeWave FGR-115RE. These radios specify a maximum range of over 90 km and can be used to form peer-to-peer

wireless mesh networks between GPS stations. Assuming the maximum range of 90 km, the absence of relay stations or repeaters and the geographical locations of the 24 GPS stations, Figure 3-1 shows the network topology of GPS stations that will be formed using the FreeWave radios. It will contain one cluster with eight nodes, one cluster with three nodes, two clusters with two nodes, and nine clusters with one node. Assuming that only one satellite uplink is required for each cluster, 13 satellite links will have to be maintained.

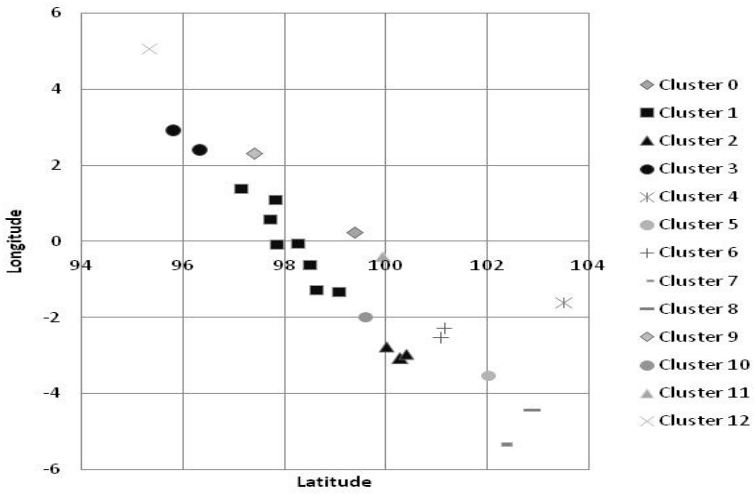

Adapted from [76]

Figure 3-1 Clusters of GPS station using 90 kilometers radio range

The range of the radio can be extended through the use of relay stations or repeaters. Thus, using the geographical locations of the 24 GPS stations, the minimum number of uplinks required and cluster size across various radio ranges can be determined. Figure 3-2 shows the number of uplinks required for the various ranges. From the figure, it can be seen that given a maximum radio range of 20 km, only two GPS stations can be linked together and all other GPS stations are out of range from each other. Therefore, 23 satellite uplinks are required in this case. However, given a maximum radio range of 250 km, all GPS stations are grouped into one cluster using only 1 uplink.

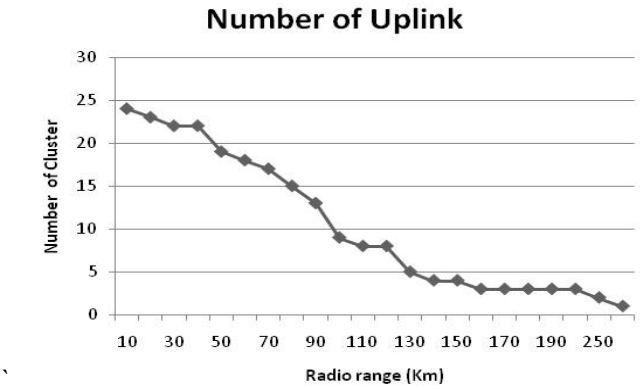

Adapted from [76]

Figure 3-2 Number of satellite uplinks required across various radio ranges

Figure 3-3 provides a graph showing the average and the maximum number of GPS stations in a cluster across a radio range from 10 km to 250 km. As the number of GPS stations in a cluster increases, the data aggregated at the cluster-head will also increase in size. This will lead to a better compression ratio at the cluster-heads and this phenomenon will be presented in more details in the following parts.

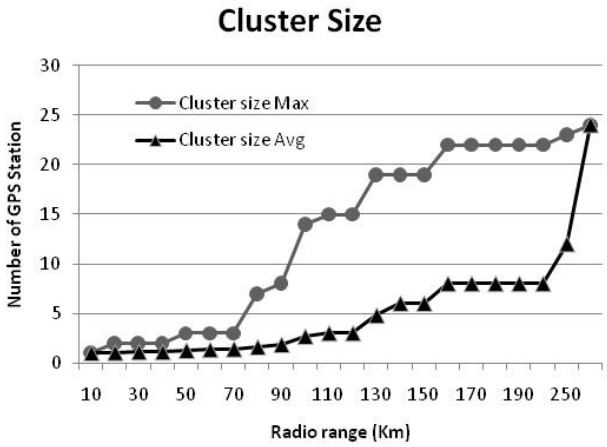

Adapted from [76]

Figure 3-3 Cluster sizes characteristics based on the various radio ranges

3.2.2. Data transmission reduction

At the time of this study, the SuGAr sent the collected data daily through dedicated satellite links from each GPS station. For this analysis, the GPS measurements will be con-

verted locally to CRINEX format at each GPS station. Figure 3-4 shows the total number of data in bytes transmitted via all the satellite links using three different setups as follows:

Setup 1: For the first setup, CRINEX data is uploaded via dedicated satellite links from each GPS station without further compression.

Setup 2: For the second setup, the CRINEX data is compressed using the LZMA algorithm prior to transmit via dedicated satellite links at each GPS station.

Setup 3: For the third and final setup, clusters of GPS stations are formed using long-range radios with various maximum transmission ranges. In each cluster, one GPS station will be designated as the cluster-head and all other stations will forward their CRINEX data to the cluster-head. The cluster-head will perform further compression using the LZMA algorithm on the aggregated data as a whole prior to transmitting the compressed data to the data server via a satellite link.

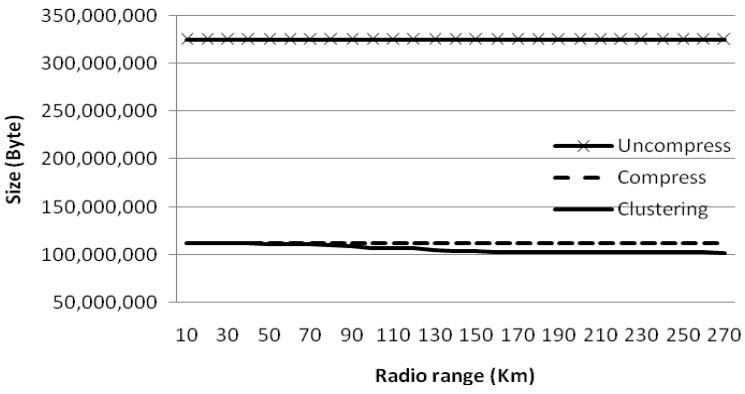

Adapted from [76]

Figure 3-4 Total size of transmitted data based on daily updates across two months for various radio ranges

From Figure 3-4, it can be seen that for Setup 2, the total number of bytes transmitted via all the satellite links over a 61 days period are reduced by about 67% when comparing to Setup 1. This demonstrates the effectiveness of the LZMA compression algorithm. Fur-

ther reduction is shown by the use of the cluster-based approach in Setup 3. In this setup, as a larger dataset is compressed, the compression ratio achieved by the LZMA algorithm at the cluster-head are more significant than in the case where compression is performed at individual GPS stations separately. Thus, this method reduces the total number of bytes transmitted by about 2% and 9% when comparing to Setup 2 for a maximum radio range of 90 km and 250 km respectively.

The analysis performs in Figure 3-4 is based on daily updates from the GPS stations. However, more frequent updates might be useful for early warning systems and near real-time assessment of tectonic plate movements. Hence, further analysis is performed to evaluate the performance of the three setups across three different update intervals: daily, hourly and two minutely. Table 3-2 is the comparison of Setup 1 (uncompressed data) and Setup 2 (un-clustered compressed data) with various update frequencies. It can be seen from the results that as the update intervals get more regular, the performance of the LZMA algorithm suffers as smaller datasets are being compressed each interval. For example, when daily updates are performed with the GPS station sampling once every 2 seconds, the dataset consisting of a total of 43200 (24hrs * 60min * 60 sec / 2) measurements (epochs) is compressed, whereas hourly updates are performed, each dataset consists of only 1800 (60 min * 60 sec / 2) measurements (epochs). However, when the updates are performed every two minutes, the use of the LZMA compression in Setup 2 still enables less data to be transmitted via the satellite links when comparing to Setup 1.

Update Frequency	**Total Transmitted Data**		
	Uncompress	**Compress**	**Percentage**[a]
Daily	325,099,037 byte	112,188,360 byte	35%
Hourly	402,298,012 byte	158,994,711 byte	40%
2Minutely	2,245,193,111 byte	979,810,017 byte	44%

a. Percentage of compress data when compare with uncompressed data

Table 3-2 Comparison of uncompressed and compressed GPS data

Figure 3-5 shows the total transmitted data size in Setup 3 as a percentage of the total transmitted data size in Setup 2 across various radio ranges. From the results, it can be seen that the use of long-range radios to form mesh networks and clusters in Setup 3 significantly reduces the amount of data to be transferred via the satellite links when comparing to Setup 2. This reduction is more significant when the update frequency increases. This is due to the use of data aggregation within the cluster to enable larger datasets to be compressed. For example, when a maximum radio range of 250 km is used, data from all 24 GPS stations will be aggregated prior to compress using the LZMA algorithm. Assuming hourly update interval, each dataset consisting of ((60min * 60 sec /2) * 24 nodes) = 43200 measurements (epochs) is compressed in Setup 3 as compares to the 1800 measurements in Setup 2. Because of this, Setup 3 manages to reduce the total data transmission across the 61 days by about 70% when comparing to Setup 2.

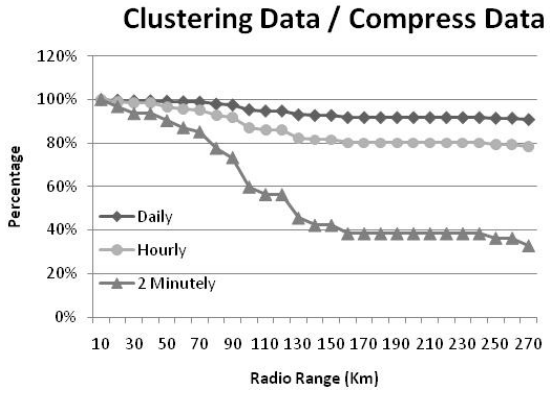

Figure 3-5 Comparing the improvement between compress observation data and use of clusters over different update intervals and radio ranges

Update Frequency	Total Transmitted Data		
	Uncompressed	Compressed	Percentage[b]
Daily	322,554,780 byte	111,317,030 byte	35%
Hourly	341,813,991 byte	137,613,065 byte	40%

Update Frequency	Total Transmitted Data		
	Uncompressed	Compressed	Percentage[b]
2 Minutely	710,381,007 byte	417,818,057 byte	59%

b. Percentage of compress data when compare with uncompressed data without header

Table 3-3 Comparison of uncompressed and compressed data without header

To further reducing the size of the transmitted data, the observation headers sent with every update from the GPS stations are removed whenever possible. This significantly reduces the size of the uncompressed data in Setup 1 as shows in Table 3-3. Moderate reductions are observed in Setup 2 when the observation headers are removed.

To conclude the evaluations, the use of Setup 3 (the use of wireless mesh networks) without observation headers is compared with Setup 2 (use of dedicated satellite links). The results of this comparison are shown in Figure 3-6. From the figure, it can be seen that the use of mesh networking, cluster-based compression and removal of the observation header significantly reduces the amount of data transmitted via the satellite links. It reduces more than 70 percent of the observation data whereas the radio range is larger than 130 km and data uploads every minute.

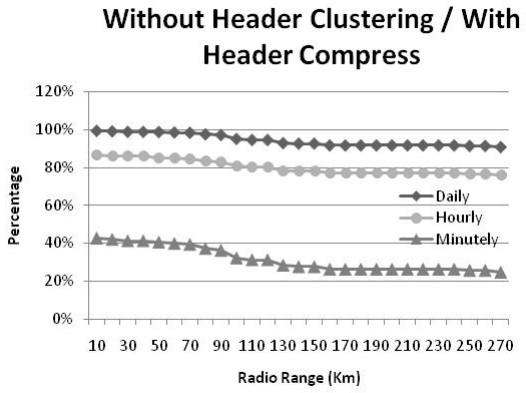

Figure 3-6 Comparing the improvement between compress observation data (with header) and the use of cluster-based compression (without headers) over different update intervals and radio ranges

3.3. Summary

In this chapter, a study of using mesh networking for GPS data compassion is presented. In which, a proposed of constructing a mesh network between GPS stations by mean of long-range radios. The mesh network could enable data aggregation and compression at cluster-head. The compressed GPS data is sent to a centralized processing server via satellite link. To evaluate the effectiveness of this method, two months data from the Sumatran cGPS array (SuGAr) is used. The result shows that the proposed use of mesh networking not only reduces the number of costly satellite uplinks required, it also significantly reduces the total amount of data transferred through these links.

CHAPTER 4

PARALLELIZING THE COMPUTATION OF GPS PROCESSING

In this chapter, computation complexity and computation time of GPS processing are calculated. Parallel GPS processing with multiple layers is proposed and studied to reduce the computation complexity and computation time of GPS stations estimated processed. By reducing the computational complexity, the proposed computation model promises to make use of small, low and spare computation power located within the cGPS network.

4.1. Computation Complexity

In-situ parallel and distributed processing of GPS corrections can be made possible using mesh networking. The observation data from adjacent GPS stations can be grouped together and processed in a hierarchical fashion. Compared to the conventional methods of sequential processing, the computational complexity and computation time of parallel and distributed GPS processing with various schemes decrease significantly. By sharing data within the mesh network, it is possible for in-network processing to be performed for GPS corrections using the processing capability of embedded system at each GPS station. This allows early-warning applications to be developed without the need for costly data trans-

mission to a remote centralized server. The remaining of this section is organized as follow. First, GPS measurements and parameters estimation process are briefly presented. Next, the computational complexity of parallel processing is evaluated using single layer and multiple layers approaches. Finally, two empirical experiments with various settings are studied.

Assuming that all receivers can receive signals from both frequencies L1 and L2, the ionosphere-free linear combination could be calculated. The distance between satellites and receivers is given by carrier-phase and pseudo-range measurements. In phase measurement, at time t, the distance between the receiver r and the transmitter x is derived as follow

$$L_{rxt} = \rho_{rxt} + b_{rxt} + z_{rt} m(\theta_{rxt}) + \omega_{rxt} + C_{rt} + c_{xt} + v_{rxt} \quad (4.1)$$

and the pseudo-range measurement is derived as

$$P_{rxt} = \rho_{rxt} + z_{rt} m(\theta_{rxt}) + C_{rt} + c_{xt} + \eta_{rxt} \quad (4.2)$$

in which, ρ_{rxt} is the true range, b_{rxt} is the phase bias or ambiguity, z_{rt} is the zenith troposphere delay, $m(\theta_{rxt})$ is the map function of elevation angle between transmitter and receiver. Receiver and transmitter corrections are C_{rt} and c_{xt} respectively. The noise of the measurement is represented by v_{rxt} for phase and η_{rxt} for pseudo-range measurement.

The observation data is considered from R receivers and X transmitters spanning across Δ time (typically Δ equal to 24 hours) with the data collection frequency σ. The median probability that a satellite signal is detected by a receiver above an elevation cutoff angle (the minimum satellite elevation angle above the horizon) is given by $\Omega/4\pi$ (≈ 0.25 at 15° cutoff). Thus, the number of measurements is given by

$$m = RX\ (\Omega/4\pi)\ (\Delta/\delta)\ d \quad (4.3)$$

Whereby d is the number of data types, typically including two types: ionosphere-free phase and pseudo-range. The number of parameters from those receivers and transmitters will be estimated and these consist of receivers, transmitters and polar motion parameters. It is given by

$$n = aR + bX + c \tag{4.4}$$

The parameters related to a receiver include three Cartesian coordinates, tropospheric delay, receiver clock bias and phase bias parameters for each transmitter in the view of that receiver, so a = 5 + X. The transmitter parameters include epoch state position, velocity, two solar radiation parameters, Y bias parameter and clock bias, b = 10. Polar motion and rates estimated in one day time is given by c = 5.

The computational complexities of the parameter evaluation process using least square estimate method of n parameters with m measurements require the number of arithmetic operations B in equation (4.5). This is also known as the computational burden. The detail analysis could be found in Zumberge, et al [26].

$$B \propto n^2 m \tag{4.5}$$

One approach to reduce the computational complexity is to divide the data into groups and layers, which could process in parallel fashion. In addition, it makes use of common parameters and receivers between groups in the same layer. The detail of this processing approach will be presented in the next sections.

4.2. Parallel GPS Processing

In this part, estimation of parallel parameters is studied with the objective of reducing computational complexity and processing time when comparing to the centralized processing method. It deals with estimating n unknown parameters of m measurements from R

receivers and X transmitters. Moreover, receivers are divided into groups based on criteria such as antenna type [82], geography [83], and/or availability of data. Groups may share some common references stations/receivers. Single layer and multilayer parallel processing approaches will be presented in the remaining of this section. All used notations are listed at the end of this chapter.

4.2.1. Single layer parallelism

In single layer method, receivers are divided into J computation groups (Figure 4-1) instead of estimating all parameters within one group. Suppose that the number of common parameters between all groups is κn and the remaining parameters which equally divided for each group is (1- κ)n/J. In addition, number of common reference receivers between all groups is ζR. For simplicity, suppose that the number of common measurements proportional to ζ is given by ζm and the remaining measurements are equally divided between groups, i.e. (1 - ζ)m/J, for each group. Number of parameters and measurements at level zero for each group is thus derived as

$$n_{0,i} = \kappa n + \frac{(1-\kappa)n}{J} \text{ and } m_{0,i} = \zeta m + \frac{(1-\zeta)m}{J} \tag{4.6}$$

Arithmetic operations required are proportional to $n_{0,i}^2 m_{0,i}$. From equation (4.5)

$$B_{0,i} \propto \left(\frac{(1+(J-1)\kappa)n}{J} \right)^2 \frac{(1+(J-1)\zeta)m}{J} \tag{4.7}$$

where $B_{0,i}$ is the number of arithmetic operations required at any group i ($1 \le i \le J$) at level zero. There are J groups in this level with the same number of arithmetic operations, so the total operation is equal to J multiplied by the number of operation of one representative group $B_{0,1}$. Hence, total number of arithmetic operations at level zero is equal to

$$B_0 = \sum_{i=1}^{J} B_{0,i} = J * B_{0,1} \tag{4.8}$$

Finally, the parameter estimation processing at level 1 is the refinement of J group at level zero as shown in Figure 4-1. It includes n parameters and the number of measurements equaling to the total number of estimated parameters of J groups at level zero. As equation (4.5), the computational burden at level one is

$$B_1 \propto n^2 \sum_{i=1}^{J} n_{0,i} = n^2 \left(1+\left(J-1\right)\kappa\right) n \tag{4.9}$$

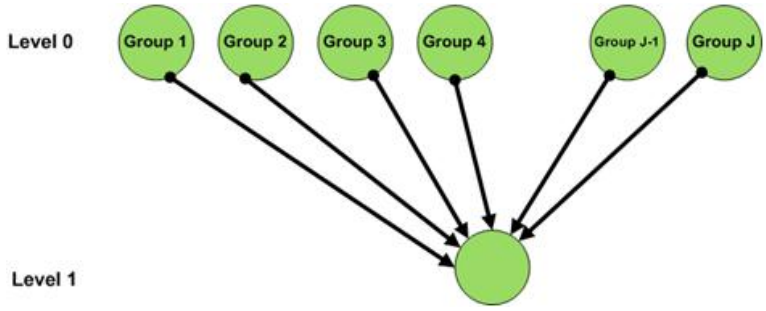

Figure 4-1 One level parallel processing

Therefore, the total number of operations B is equal to the sum of all computational burdens at level zero and level one are given as

$$B = B_0 + B_1 \propto n^2 (1+(J-1)\kappa)\left(\frac{(1+(J-1)\kappa)(1+(J-1)\zeta)m}{J^2} + n\right) \tag{4.10}$$

The computational reduction percentage χ is equal to the number of operations divide by the number of operation n^2m required for simultaneous parameter evaluation.

$$\chi = \frac{B}{n^2 m} \propto (1+(J-1)\kappa)\left(\frac{(1+(J-1)\kappa)(1+(J-1)\zeta)}{J^2} + \frac{n}{m}\right) \tag{4.11}$$

The value of χ approaches unity when both ζ and κ approach 1 assuming n/m is small. Hence, if all the parameters and receivers are common between groups, parallel processing is ineffective.

This method is applied for the Sumatra continuous GPS (cGPS) array [76] and the results are evaluated for two different configurations using the parameters X = 24, $\Omega/4\pi$ = 0.25, Δ = 24h, σ = 2 min, d = 2, a = 29, b = 10, and c = 5. For the first configuration, the number of receivers R equals 40 which includes 32 GPS stations of Sumatra cGPS array and 8 International GNSS Service (IGS) reference stations. In the second configuration, only 32 Sumatra cGPS stations are used without any reference station.

In the first configuration, ζ equals to the number of reference stations divide by the total number of stations, so, ζ=8/40=0.2. The number of common parameters equals to the sum of the parameters of the common reference stations, the transmitter parameters and the polar motion. This can be calculated using equation (4.12), we have $\kappa \approx 0.34$.

$$\kappa n = a\zeta R + bX + c \tag{4.12}$$

In the second configuration, the number of common reference stations, ζ, is equal to zero and so, using equation (4.12) thus $\kappa \approx 0.17$.

The computational reduction with respect to the different number of groups is presented in Figure 4-2. In the case where reference stations are utilized, the maximum reduction reached 57% when receivers are divided into 5 groups. It decreases when the number of group increases due to the overheads of the reference stations when using more groups. In the case where no reference stations is used, the maximum reduction reaches 91.6% when receivers where divided into 16 groups with 2 receivers per group in Figure 4-2.

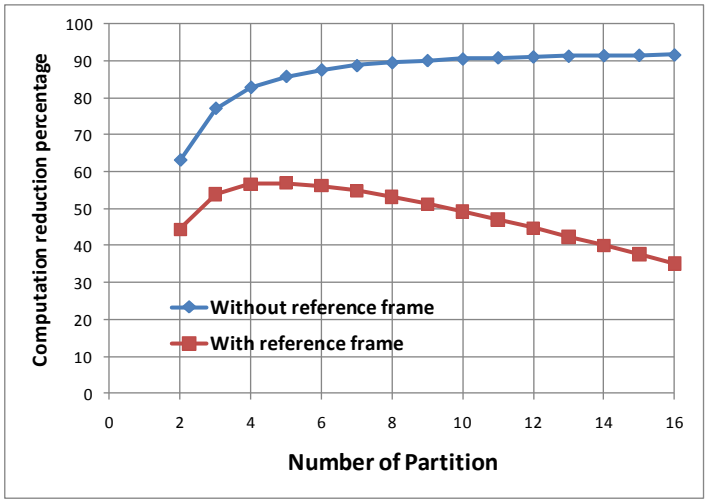

Figure 4-2 Computational reduction of Sumatra cGPS array using one level parallel processing

4.2.2. Multilayer parallelism

For generalization, multilayer parallel is studied with L layer such that each layer includes power of p groups. It means that there are p power of L groups at level zero and each group at level j (1≤j≤L) receives data from p groups at adjacent predecessor level j-1. For instance, p is equal to two in Figure 4-3.

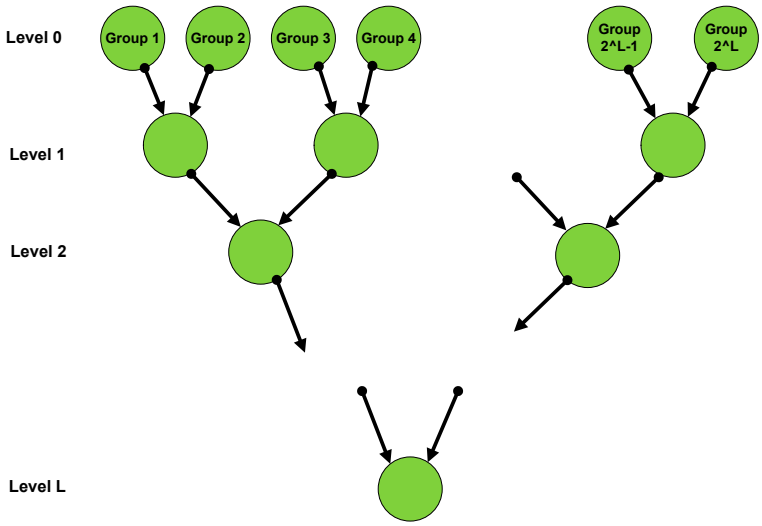

Figure 4-3 Multilayer parallel processing with L layer with power of 2 groups.

In Figure 4-3, the processing tree will contain $2^{\wedge L}$ groups at level 0 and each group at level j (1<j≤L) is the combination of 2 nodes at level j – 1. With the same assumptions of

common parameters and measurements with the single layer parallel method mentioned above, the number of parameters is equal to the sum of common parameters and private parameters of each group of receivers and the number of measurements is equal to the sum of common measurements from common receivers and private measurements from private receivers.

$$n_{0,i} = \kappa n + \frac{(1-\kappa)n}{p^L} \text{ and } m_{0,i} = \zeta m + \frac{(1-\zeta)m}{p^L} \tag{4.13}$$

Therefore, the number of arithmetic operations of group i at level zero is

$$B_{0,i} \propto n_{0,i}^2 m_{0,i} = (\kappa n + \frac{(1-\kappa)n}{p^L})^2 (\zeta m + \frac{(1-\zeta)m}{p^L}) \tag{4.14}$$

So the total computational burden for level zero which include p^L group is given by

$$B_0 = \sum_{i=1}^{p^L} B_{0,i} \tag{4.15}$$

Furthermore, the computational burden for each group i at level j ($1 \le j \le L$) is proportional to $n_{j,i}^2 m_{j,i}$, in which the number of parameter $n_{j,i}$ is equal to the sum of common parameters κn and the private parameters of p ancestor groups at level j–1, each of which comprise of $\left((1-\kappa)n * p^{j-1}\right)/p^L$ private parameters. Therefore,

$$n_{j,i} = \kappa n + \frac{(1-\kappa)n}{p^L} p^j \tag{4.16}$$

In addition, the number of measurements at level j is equal to the summation of all estimated parameters of p ancestor at level j–1,

$$m_{j,i} = \mathrm{p}(\kappa n + \frac{(1-\kappa)n}{p^L} p^{j-1}) = \mathrm{p}\kappa n + \frac{(1-\kappa)n}{p^L} p^i \tag{4.17}$$

Therefore, the computational burden of each group i at level j is proportional to

$$B_{j,i} \propto (\kappa n + \frac{(1-\kappa)n}{p^L} p^j)^2 (p\kappa n + \frac{(1-\kappa)n}{p^L} p^j) \tag{4.18}$$

The total computational burden for level j which include p^{L-j} groups is then derived as

$$B_j = \sum_{i=1}^{p^{L-j}} B_{j,i} \propto (\kappa n + \frac{(1-\kappa)n}{p^L} p^j)^2 (p\kappa n + \frac{(1-\kappa)n}{p^L} p^j) p^{L-j} \tag{4.19}$$

The total computational burden of multiple levels parallel processing method is equal to summation of computational burden of all levels from level 0 to L as follows:

$$B = \sum_{j=1}^{L} B_j + B_0 \propto \sum_{j=1}^{L} (\kappa n + \frac{(1-\kappa)n}{p^L} p^j)^2 (p\kappa n + \frac{(1-\kappa)n}{p^L} p^j) p^{L-j} + (\frac{(1-\kappa)n}{p^L} + \kappa n)^2 (1 + (p^L - 1)\zeta) m \tag{4.20}$$

4.2.3. Computation time

Assuming the computation time is the dominant latency between processing groups in adjacent layers. In the worst case, the processing time of parallel GPS processing is calculated by the summation of the maximum computation time at each layer. Those groups required most computation time at each layer would form a critical computation path. The critical path for the single layer and multilayer parallel process as is given in Figure 4-4 and Figure 4-5 respectively.

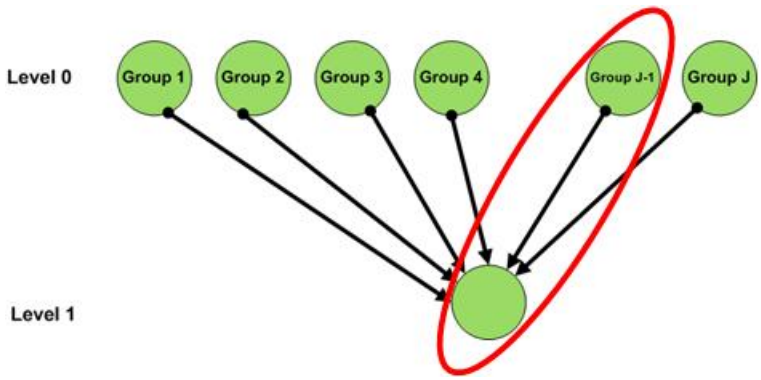

Figure 4-4 Single layer critical path

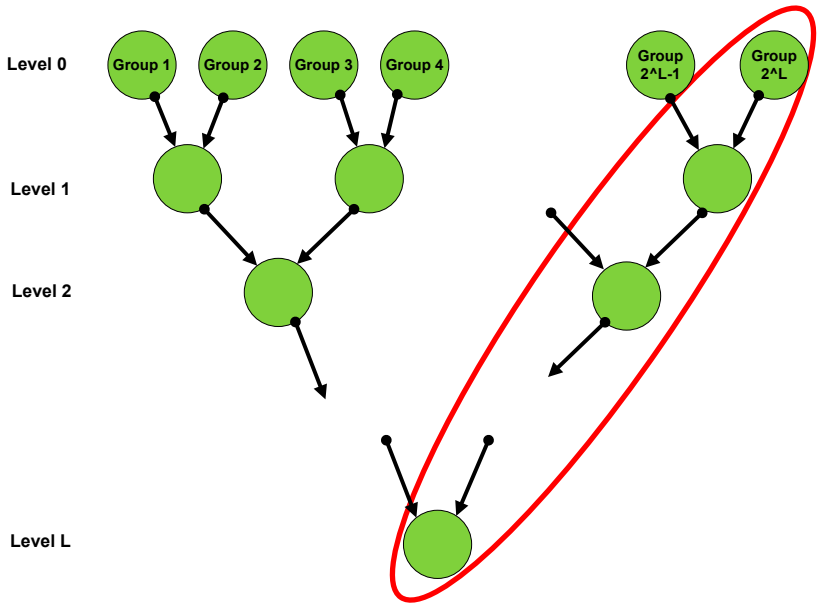

Figure 4-5 Multilayer critical path

The computation time C is equal to the number of arithmetic operations multiplied by c, the computation time for one arithmetic operation. The equation for single layer and multilayer methods are therefore derived as follows

$$C_{onelayer} = \left(n^2 \left(1+\left(J-1\right)\kappa\right)n + \left(\frac{(1+(J-1)\kappa)n}{J} \right)^2 \frac{(1+(J-1)\zeta)m}{J} \right) * c \tag{4.21}$$

$$C_{multilayer} = \left(\sum_{j=1}^{L} \left(\kappa n + \frac{(1-\kappa)n}{p^L} p^j\right)^2 \left(p\kappa n + \frac{(1-\kappa)n}{p^L} p^j\right) + \left(\frac{(1-\kappa)n}{p^L} + \kappa n\right)^2 \left(1+(p^L-1)\zeta\right) \frac{m}{p^L}\right) * c \tag{4.22}$$

4.3. Empirical Study

To compare the reduction in computational burden and computation time of single layer and multilayer parallel parameter estimation for GPS processing, two experimental setups are studied.

Experiment set 1: In this experiment, the network parameters estimate does not include reference receivers. This experiment compares number of processing groups, compu-

tation reduction and computation time between three system settings with different number of GPS receivers. They are

- Single layer,
- Multilayer with power of 2,
- Multilayer with power of 3.

The results of experiment set 1 are shown in Figure 4-6, Figure 4-7, and Figure 4-8. From the result, it can be seen that when the number of receivers equal to 16 or 48 with multilayer power of 3 method, the number of computation process is the lowest and the computer reduction is lower than other settings. However, the computational burden of it is larger than multilayer with power of 2. When number of receivers are larger than 48, the computation reduction is almost analogous for all settings. Parallel GPS processing significantly reduces the computation complexity, especially when the number of receivers is bigger than 32. Furthermore, multilayer processing significantly reduces the computation time by about 50% when compared with the single layer approach. In most of the cases, the number of computation processing of multilevel methods is lower than one level method. As the result, multilevel is the best selection for in-network parameter estimation processing as demonstrated in this experiment.

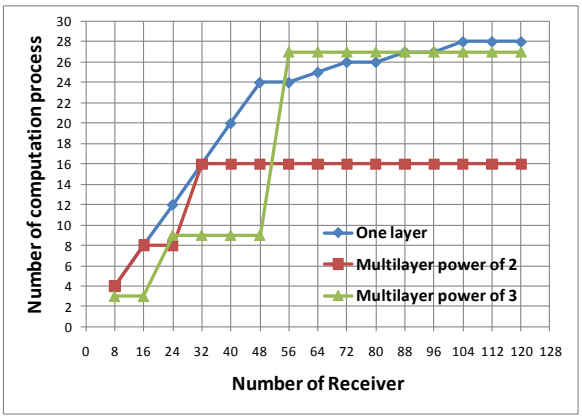

Figure 4-6 Comparison number of computation processing groups

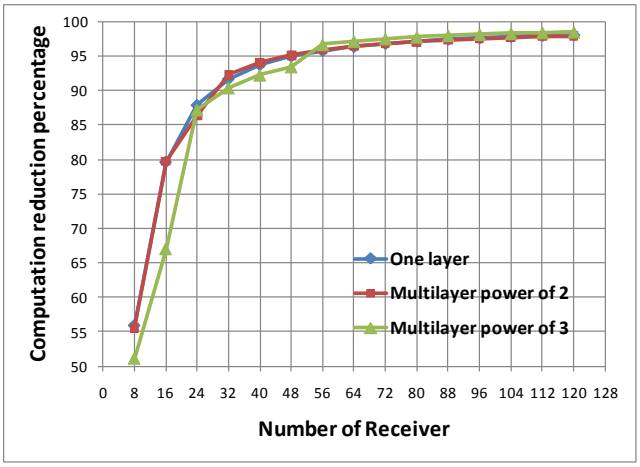

Figure 4-7 Comparison of computation reduction

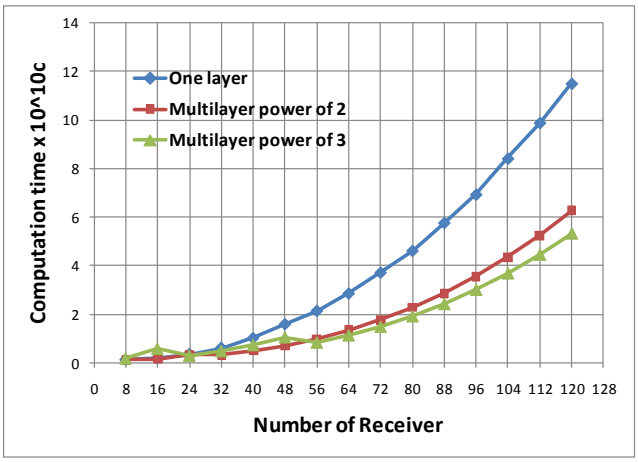

Figure 4-8 Comparison of computation time

Experiment set 2: Global parameter estimation with eight reference receivers (all groups will share the same eight reference receivers) using the same three comparative settings as the first experiment:

- Single layer,
- Multilayer with power of 2,
- Multilayer with power of 3.

The experimental results are shown in Figure 4-9, Figure 4-10 and Figure 4-11 (reference receivers are not included in the number of receivers shown in x-axis).

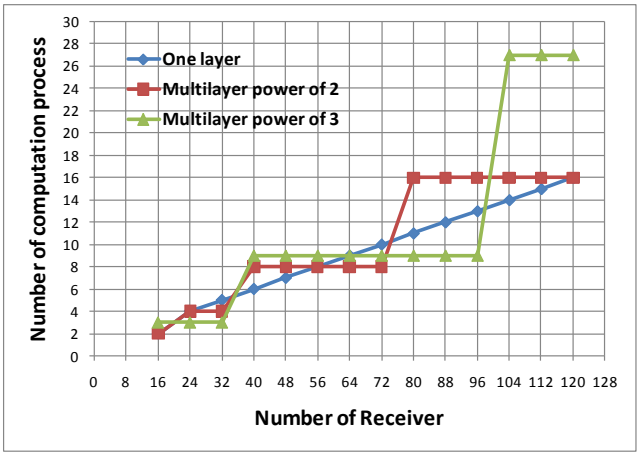

Figure 4-9 Compare the number of computation processing groups

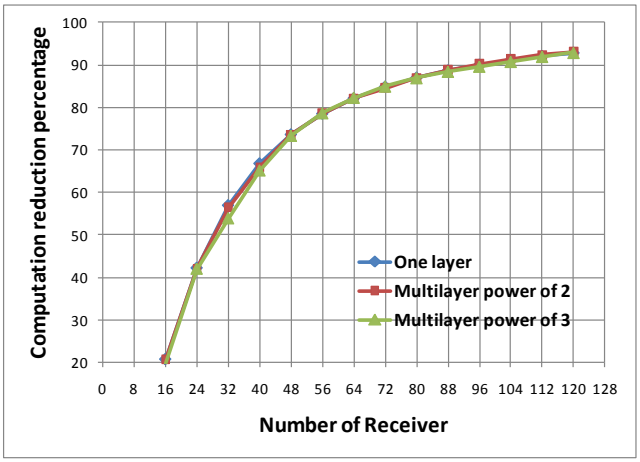

Figure 4-10 Compare the computation reduction

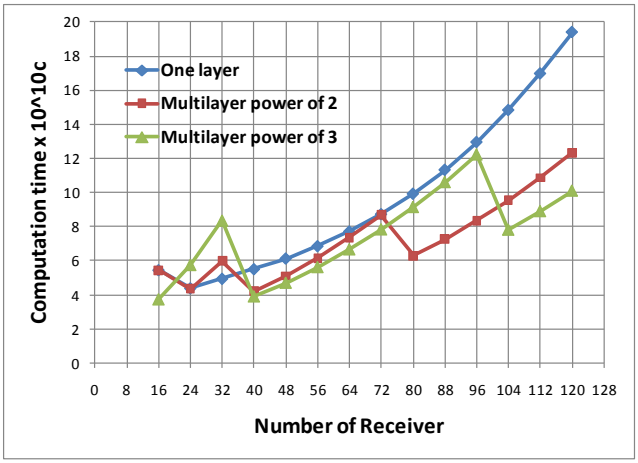

Figure 4-11 Computation time comparison

From the results, it can be seen that when the number of receivers is equal to 32 or 96, the number of computation processes is the smallest for multilayer with power of 3. The computation reduction of this approach is also larger than the other settings in the case of 32 receivers and larger than multilayer with a power of 2 in the case of 96 receivers. Thus, it can be seen that parallel GPS processing significantly reduces the computational complexity, especially when the number of receivers is bigger than 32 and it steadily increases when the number of receivers increases. Furthermore, the multilayer processing approach slightly decreases the computation time, as in most of the cases, the number of computation processes of multilevel methods is lower than one level method.

4.4. Summary

In this chapter, a parallel and distributed method for GPS processing is presented. GPS receivers are divided into groups based on criteria such as antenna type, geographic and/or availability of the data. Groups share common parameters and reference receivers. Then they are processed in parallel, distributed and hierarchy manner. The final solution is evaluated at the bottom group in a hierarchical tree. This method significantly reduces the computational complexity and processing time.

By reducing the computational complexity, the proposed computation model promises to make use of small, low and spare computation power within the cGPS network itself, such as routers and station controllers. The dedicated wireless mesh network connection between stations is utilized to transmit and collaborative process GPS data in real-time or near real-time fashion.

Notations are used in this chapter

R	number of receiver (GPS station)
X	number of transmitter (satellite)

n	total number of parameter have to estimate
m	total number of measurement
κ	share parameters percentage between groups
ζ	share measurement percentage between groups
B	computation burden
J	number of computation group
L	number of processing level
p	in multiple level processing method, group at level i receive data from p group at level i-1
$n_{j,i}$	number of parameter at level j and group i have to estimate
$m_{j,i}$	number of measurement at level j and group i
$B_{j,i}$	computation burden at group i of level j
B_j	total computation burden at level j

CHAPTER 5

IN-NETWORK SINGLE-FREQUENCY GPS PROCESSING

In this part, in-network single-frequency GPS processing method is proposed; GPS data from Taal network is used to verify the effectiveness of the proposed method. The study focuses on long-range radio link reduction, station location error and communication bandwidth required for long-range radio uplinks.

5.1. Introduction

Active volcano deformation monitoring with GPS is carried out by establishing and operating a local network of continuous GPS receivers located on and around deforming areas [58]. In order to reduce the expenditure of constructing and maintaining the network as well as increasing coverage area of such a deformation monitoring system, single-frequency GPS receivers are utilized instead of dual-frequency GPS receivers. With single-frequency GPS monitoring system, the baseline lengths are kept less than 10 kilometers to minimize errors, which could not be estimated by single-frequency GPS data. The sort baseline network setup is widely used when monitoring a small active deformation area with dense single-frequency GPS network [13, 58, 59]. In such a small deformation monitoring network, the tropospheric and the ionospheric delay between two receivers are

nearly zero, therefore they do not effect on the baseline processing results [14]. Furthermore, orbit bias over such short distances could be ignored [84].

The proposed in-network single-frequency GPS processing method is designed for a small coverage and mix-mode GPS network with WMN connection between stations. The WMN is utilized to exchange raw GPS data, estimated corrections, control data, and processing results. In these types of mix-mode GPS network, most of stations are equipped with single-frequency receiver and only some of them are equipped with dual-frequency GPS receiver. The network is installed around an active volcano or a tectonic plate. Four processing proposed steps of distributed GPS processing are described as following.

- **Step 1:** GPS data from dual-frequency stations in the mix-mode GPS network are processed with dual-frequency reference stations in the area to estimate the long time velocity. The process results constraint dual-frequency stations in the network with references stations around the deformation area, which are not affected by deformation activities. The data could be processed at a station inside the mix-mode network or at an observation center is located outside of the mix-mode network.
- **Step 2:** One or more dual-frequency stations are selected as reference station for the network. It bases on criteria such as data availability, station location or deformation activity around selected stations.
- **Step 3:** The remaining single-frequency stations and dual-frequency stations of the network are clustered by criteria such as station location, antenna type or data availability. A point-to-point mesh network is constructed and connected all stations belong to each cluster. One station in a cluster is selected as cluster head. All mesh networks are connected with reference stations and centralized

server to exchange or broadcast GPS data, estimated corrections and control commands.

- **Step 4:** Single-frequency GPS data is processed at cluster head by utilizing mesh network to send raw GPS data from stations in each cluster including reference stations to their cluster head. The velocity of dual-frequency stations estimated in step 1 is used as known parameters. The estimated stations movements of the remaining station could be utilized to trigger pre-defined actions when the movement of a station or number of stations in the network exceeds a pre-defined threshold.

To evaluate the efficiency achieved by proposed in-network single-frequency GPS processing, station's location estimation is performed using the archived Taal GPS network data in the next parts.

5.2. The Taal GPS Network

Taal GPS network (Figure 5-1) was installed around Taal Volcano, a complex stratovolcano located on the island of Luzon in the Philippines, about 50 km south of Manila. The Taal volcanic system consists of a volcano island with 5 km in diameter located within the large area of Taal Lake, about 20 km by 25 km area. This network included four dual-frequency sites and fourteen single-frequency sites, making it one of the densest volcanoes monitoring system in the world. Three out of four dual-frequency sites were installed in May 1998 including KAYT, TVST, and PINT. These sites were installed approximately the same distance from the volcano's center, on opposing flanks of Volcano Island. In 2001, the last dual-frequency site was installed on a mountain near Tagaytay highway outside of Lake Taal area, TGYT site. In June 1999, twelve L1 sites were installed, eight of them (TV01, TV02, TV03, TV04, TV05, TV06, TV07, and TV12) were installed on Volcano Island, with four additional sites (TV08, TV10, TV11, and TV13)

were installed around the caldera's rim. The last two sites were installed in March 2001 (TV14 and TV15). All sites of Taal GPS network were retired on July 2005. The single-frequency carrier-phase and pseudo-range measurements were continuously transmitted to a central computing facility thought TDMA radio by line of sight communication using FreeWave radio modem. The detail instruments and operations of Taal GPS network could be found in [13].

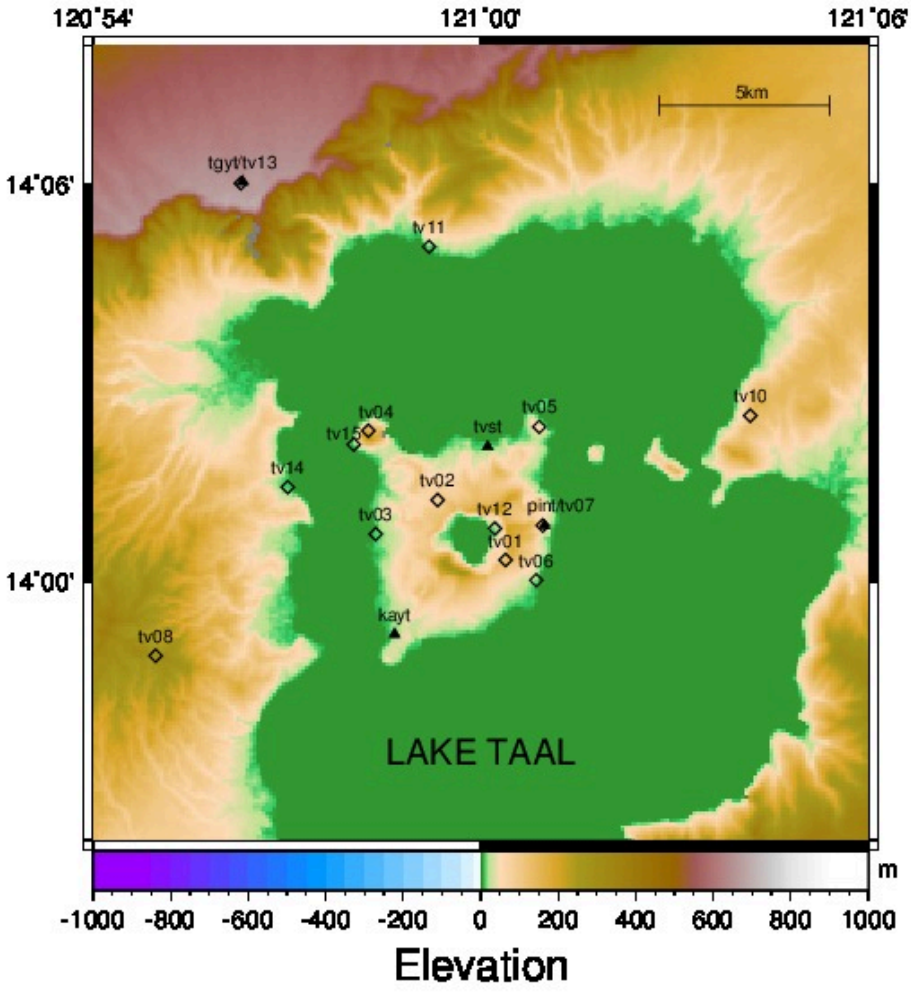

Figure 5-1 Elevation map of Taal Volcano with entire Taal GPS network. Dual-frequency GPS sites are shown as solid triangles; single-frequency GPS sites are shown as open diamond.

5.3. Process Taal's Dual-Frequency GPS Data

In Step 1, four dual-frequency sites in Taal GPS network are processed together with thirteen reference stations around the deformation area to estimate location and ve-

locity of Taal's dual-frequency stations. Those reference stations provide reference to region frame, which are not affected by volcano deformation activities. The data could be processed using the immediately available IGS ultra-rapid orbit prediction for precise orbits and satellite clocks and subsequently reprocessed using more precise products such as IGS rapid products or IGS final products for precise orbits, satellite clocks and station clocks when they are available. The results present in Figure 5-2 and Figure 5-3 utilizing IGS final product. GPS data are processed in a standard sequence including cycle-slip screening and outlier removal, troposphere estimation, ambiguity resolution, and network solution for daily site coordinates. The estimated Taal's dual-frequency stations location and velocity from 1998 to 2005 are shown in Figure 5-2 and Figure 5-3 respectively.

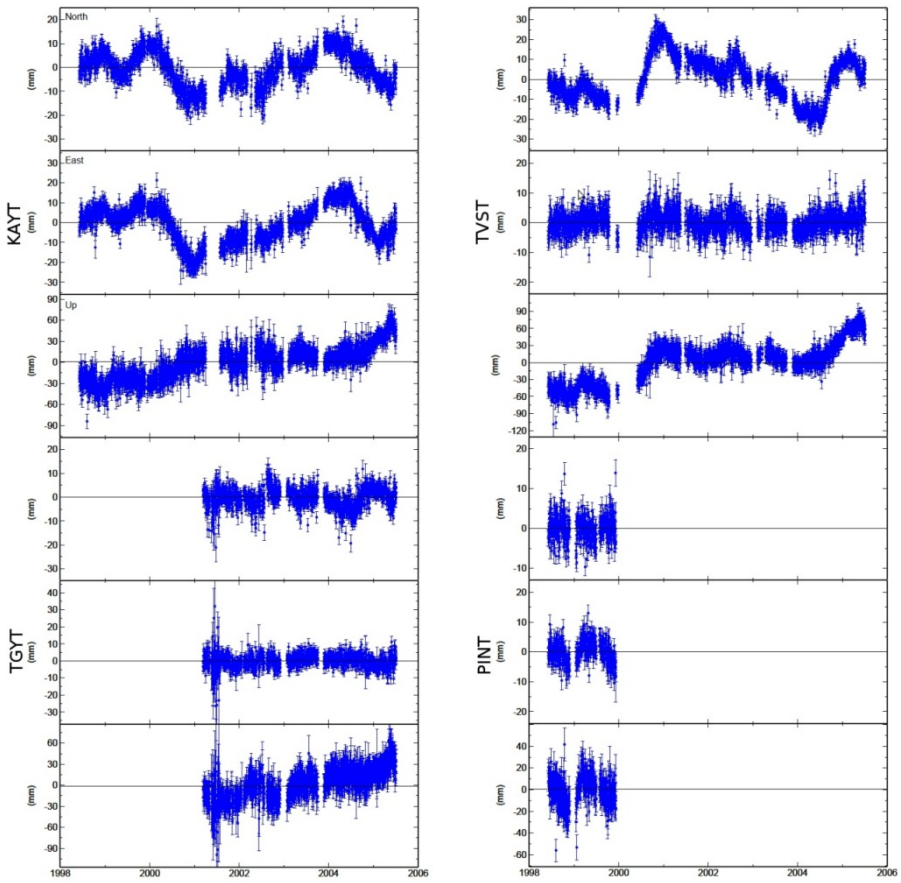

Figure 5-2 Taal's dual-frequency GPS stations location

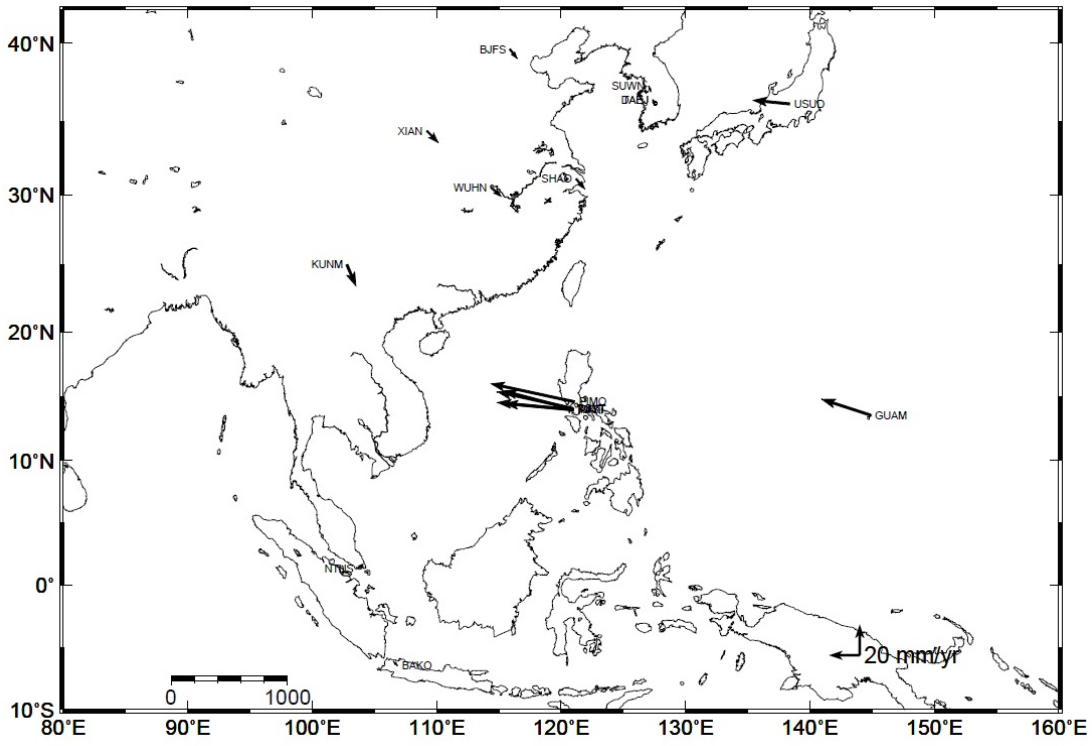

Figure 5-3 Taal's dual-frequency stations and reference stations velocity

5.4. Centralized Single-Frequency Taal's GPS Data Processing

The comparison between proposed in-network distributed and centralized single-frequency processing method is presented in this part. In which, all L1 data from all stations in Taal GPS network (including data from four dual-frequency stations) are processed together for daily coordinate solutions with baseline referenced to KAYT station, which has the longest data spanning as in step 2 of the proposed processing method. KAYT station velocity estimated in previous part is used as known parameters. Data are processed in a standard sequence including cycle-slip screening and outlier removal, ambiguity resolution, and a network solution for daily site coordinates. The time series of all stations from July 2001 to June 2005 are shown in Figure 5-4. In this figure, baseline length increases from 2.8 km at TV03 station to 13.3 km at TGYT station. For clarity, coordination changes of each station are placed 100 mm separate from each other in Y-axis of Figure 5-4.

It can be seen that the scatter in the vertical component is double the scatter of horizontal components for all stations and it increases almost linearly with increasing baseline length. The scatter in north component is slightly higher than the scatter in east component. The processing result of dual-frequency stations in Figure 5-4 agrees with the result of dual-frequency GPS data in previous part and processing results in [13] when early collected data of Taal GPS network are processed. The larger movements in east component scatter of single-frequency coordinate estimation in Figure 5-4 is probably the result of small-scale ionospheric effects at low latitudes (Taal's GPS stations are around 14^0N).

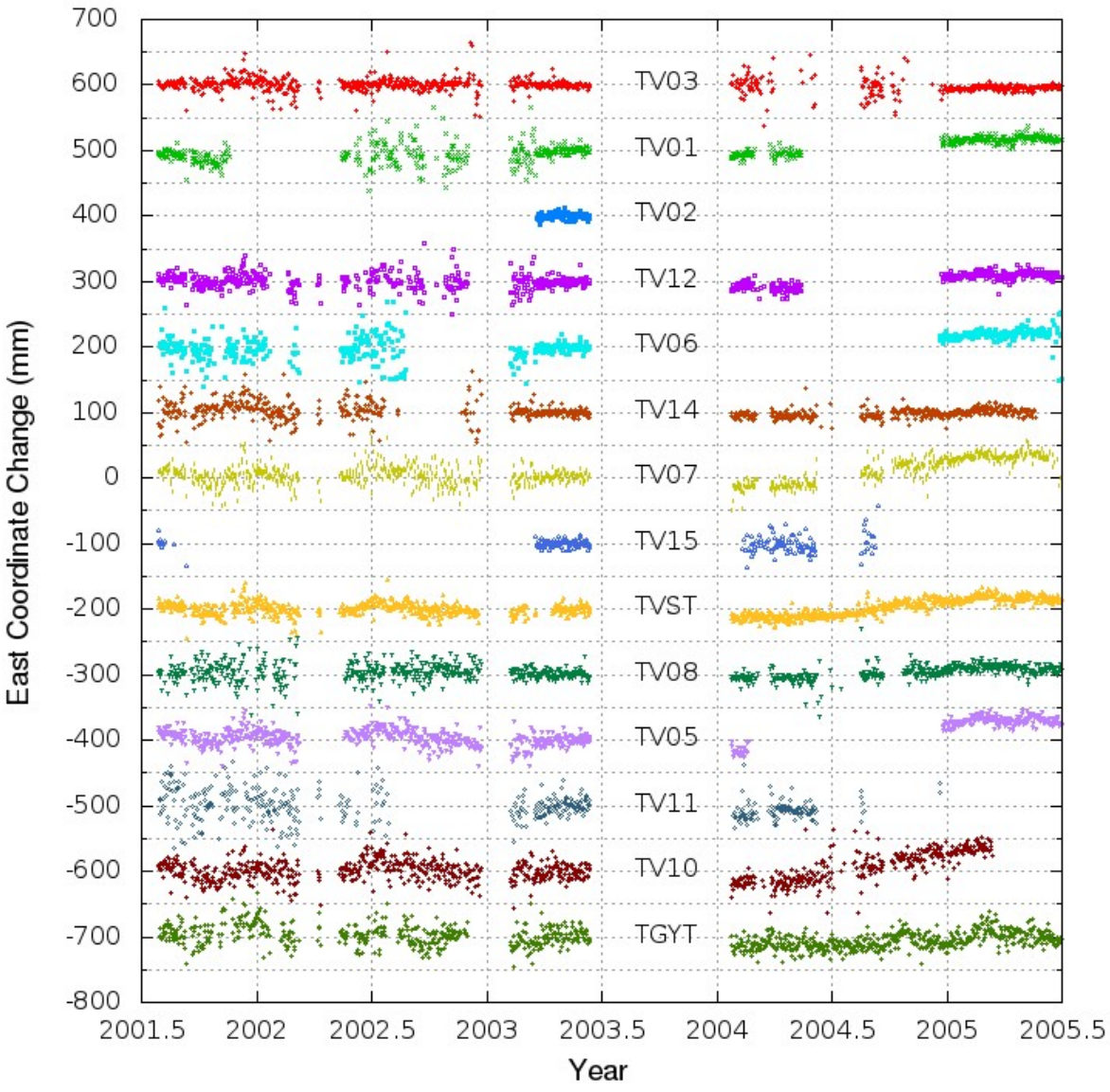

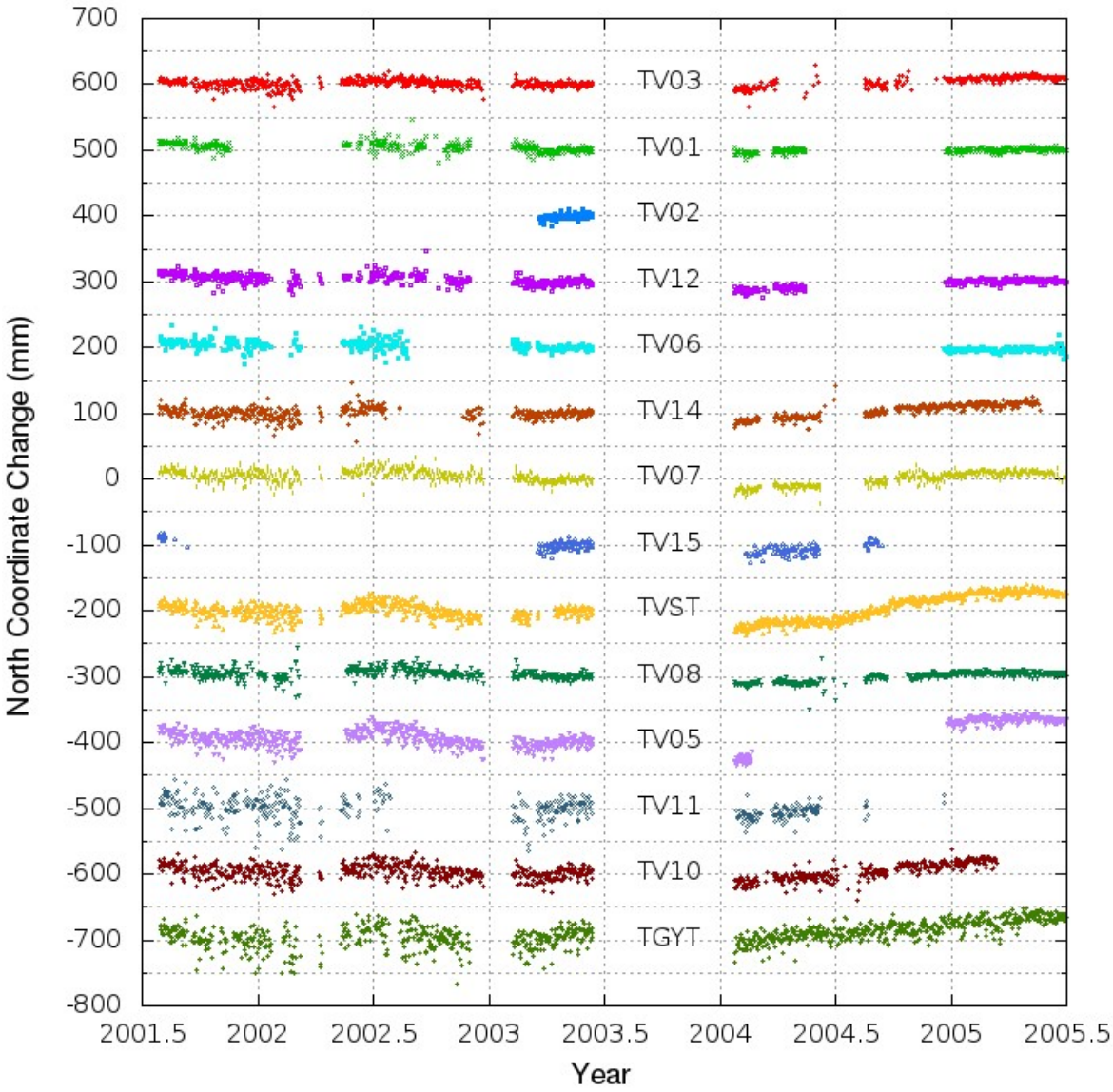
North Coordinate Change (mm)
700
600
500
400
300
200
100
0
-100
-200
-300
-400
-500
-600
-700
-800
2001.5
2002
2002.5
2003
2003.5
2004
2004.5
2005
2005.5
Year
TV03
TV01
TV02
TV12
TV06
TV14
TV07
TV15
TVST
TV08
TV05
TV11
TV10
TGYT

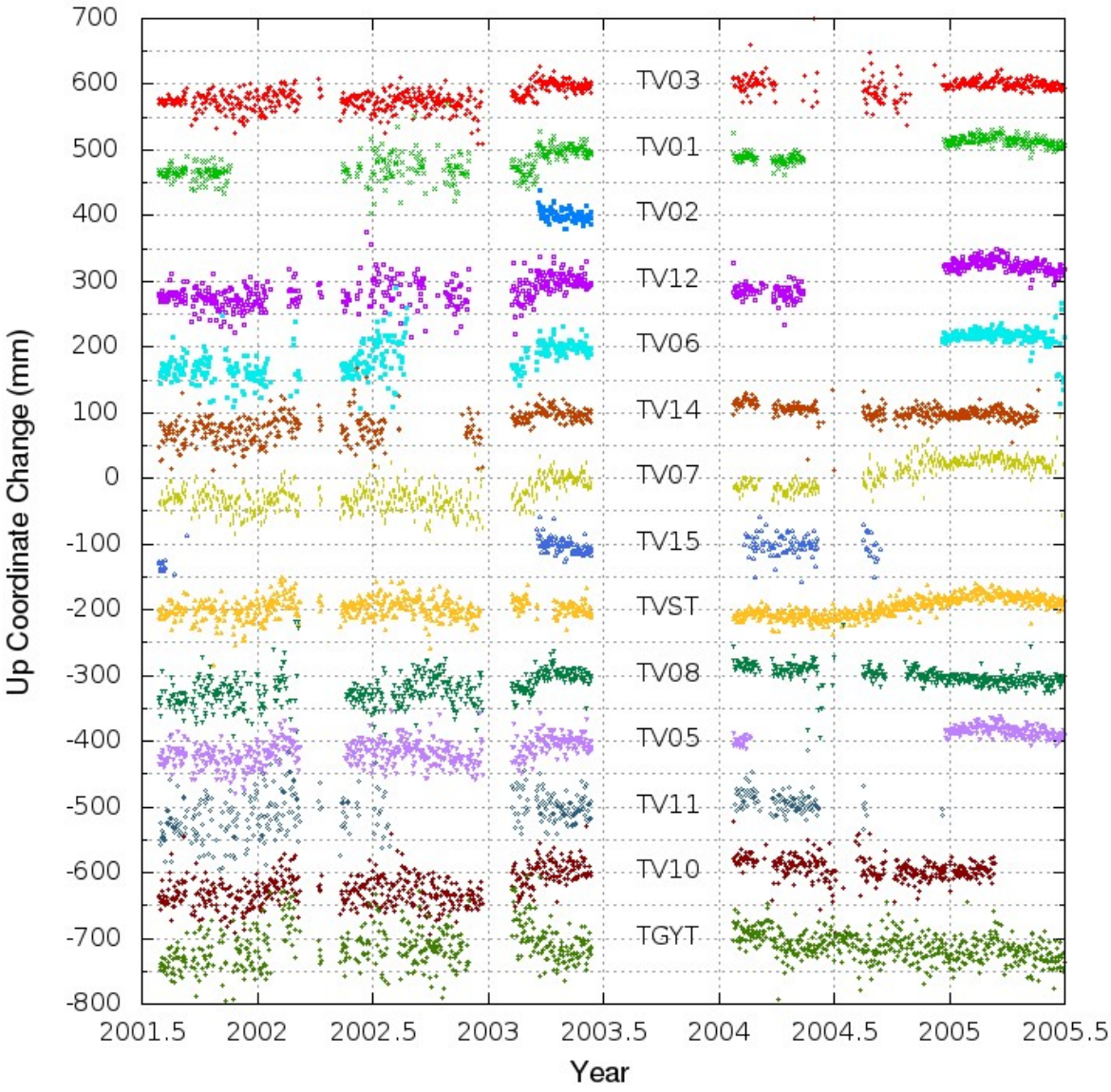

Figure 5-4 Time series of all single-frequency stations coordination

5.5. WMN for Taal Single-Frequency GPS Processing

To analyze the optimization achieved by the use of mesh networking using proposed processing method on the Taal GPS data, performance evaluation is studied by using the single-frequency archived Taal observation data for 84 days (from day 80 to day 163) of year 2003. Only 15 stations are taken into account in this case study, as only they are able to provide the almost complete GPS dataset for the entire period. This experimental dataset could be found at UNAVCO data archive website [85]. Relative positions of stations in the network are estimated on baselines referenced to KAYT station.

The assumptions made for the evaluations presented in this study are as follows

- All GPS stations have enough energy to deal with overheads caused by the additional communication equipments and the data computation required. This assumption can be satisfied by adding more batteries and solar panels to the existing station or making use of existing harvested energy by replacing long-range radio with one or more shorter-range radios.
- The transmission overheads for wireless communication, such as packet formatting and control protocols, are not included in the evaluation because they will not have significantly impact on the analysis presented in this study.

The three main performance attributes of interest in this study are the reduction of the number of long-range radio upload links, stations location errors, and communication bandwidth required of WMN's links.

5.5.1. Uplinks reduction

Instead of communicating with centralized observatory station by using a dedicated very long-range and high power consumption FreeWave radio, each GPS station can be equipped with one or more shorter range and lower power consumption radios such as the XBee-Pro XSC, 900 MHz long-range RF module. These radios specify a maximum range of over 9.6 km and can be used to form peer-to-peer WMN between GPS stations. Our study shows that a maximum range of 6 km is required to connect two near by stations in Taal network, which is well within the maximum LoS range of the XBee-Pro XSC RF module. As the result, the network contains only one cluster of fifteen nodes. Supposing that only one long-range radio is required for the cluster to upload all the observation data to the centralized server, only one long-range radio will have to be maintained in this WMN setup.

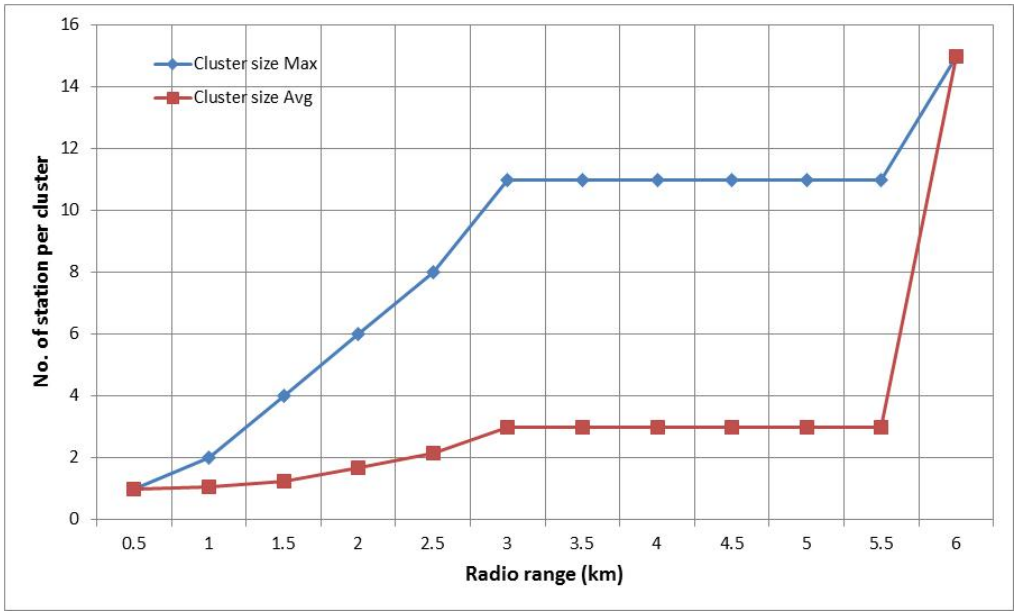

Figure 5-5 Cluster sizes characteristics based on the various radio ranges

Radio range can be extended with relay stations or repeaters to overcome obstructions. Thus, using the geographical locations of Taal's 15 GPS stations, the minimum number of uplinks is required and cluster size across various radio ranges can be determined. Figure 5-5 provides a graph showing the average and the maximum number of GPS stations in a cluster with radio range from 0.5 km to 6 km. From the figure, it can be seen that given a maximum radio range of 0.5 km, only two GPS stations can be connected with each other and all other GPS stations are out of range from each other. Therefore, 14 uplinks are required in this case. However, given a maximum radio range of 6 km, all GPS stations are grouped into one cluster using only one uplink.

5.5.2. Stations location errors evaluation regardless communication channel errors

In this part, two experiments are studied with various radio range settings and sampling rates without considering communication channel errors rate. The estimated stations location are compared with the results using centralized single-frequency GPS processing, when GPS data from all stations in Taal's network are available as in section 5.4. KAYT station is selected as reference station for the whole network.

In the first experiment, assuming observation GPS data from the reference station is broadcasted to all stations in the network and the observation GPS data of all stations in the network is processed without any down sampling. One cluster head is selected to process data of each mesh. It can be seen from the result shown in Figure 5-6, east, north and up (ENU) errors reduce almost linearly with the increasing of radio range from 0.5 km to 3 km, therefore more stations are added into cluster when increasing radio range. ENU errors do not change when radio range increases from 3 km to 5.5 km, because the number of station in each cluster is unchanged. At 0.5 km radio range, only two stations are connected which lead to the highest stations location errors and the highest number of cluster. The horizontal components are less than 10 mm (95 % confidential) and vertical component is less than 20 mm (95 % confidential) at 3 km radio range. At 6 km radio range, all stations are grouped in one cluster. By using this network setup, all observation data could be collected and processed with the same algorithm as centralized processing method. As a result, the processing error when comparing to the centralized processing method is equal to minimum value, zero.

The results of the next experiment with various GPS data sampling rates are shown in Figure 5-7. Assume that all stations are connected with a mesh network. One cluster head is selected to process GPS data. It can be seen that the stations location errors increase when reducing data sampling rate from 30 s to 120 s. At 30 s sampling rate, the max and the min station location errors of all stations are less than 10 mm for ENU components and station location errors with 95% confidential interval are below 5 mm. The location errors increase to 30 mm when data sampling rate decrease to 120 s, and location errors at 95% confidential interval are less than 20 mm.

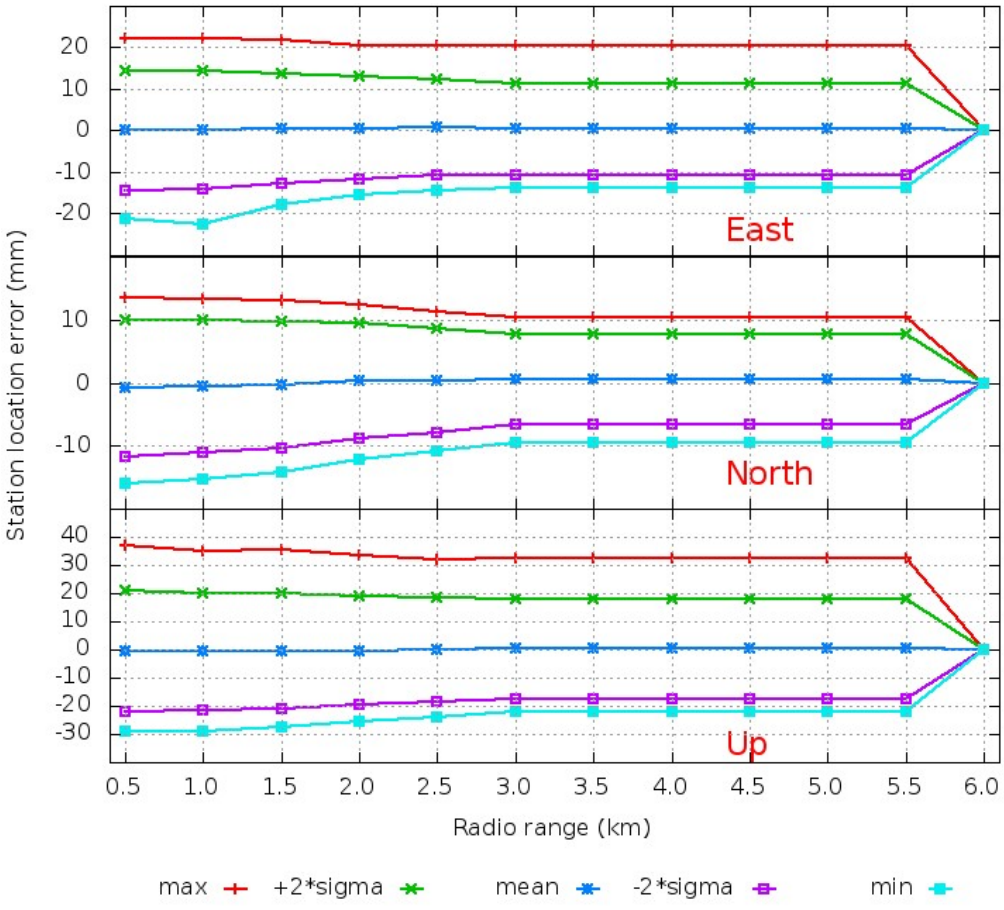

Figure 5-6 Stations location error at difference WMN radio range

Within the selected experimental period, the maximum collected station's daily observation L1 GPS data file size is 1.6 Mb at 30 seconds sampling rate and less than 300 kB for the other adjustments. The maximum bandwidth required for each radio link is 5.5 kbit/s. It could be supported by XBee-PRO XSC radio with the bandwidth up to 10 kbit/s. The maximum bandwidth is reduced by 42% and 63 % when decreasing the data sampling rate is 60 s and 120 s respectively. However, the stations location errors are nearly double when decreasing data sampling rate from 60 s to 120 s. The stations location errors are almost quadrupt when decreasing the sampling rate from 30 s to 120 s.

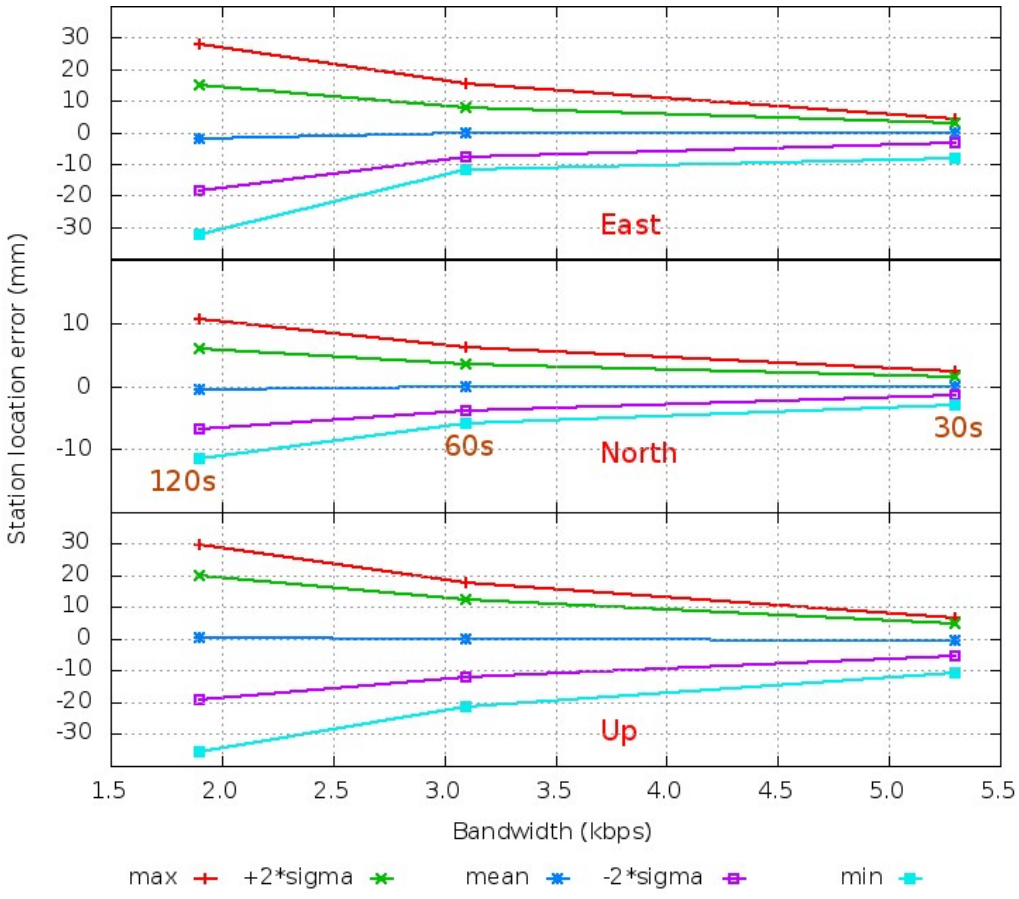

Figure 5-7 Stations locations error with respect to various radio ranges

5.5.3. Stations location errors evaluation link packet errors

In the next two experiments, terrain information and communication link's packet errors are taken into account. The estimated stations location is compared with the results from centralized single-frequency GPS processing, when GPS data from all stations in Taal network are available as in section 5.4. KAYT station is selected as reference station for the whole network.

In the first experiment, assume that the maximum radio range of 3 km could be archived without the need of relay stations or repeaters. In addition, the observation single-frequency GPS data is sampling at 30 s. Station TV03 is selected as the cluster head to keep balance between the total number of hop count of the mesh network and minimal hop count from reference station to cluster head. Hop count distribution of stations in the network is shown in Figure 5-8. It can be seen that the largest number of stations are three

hops away from cluster head. Reference station is one hop from cluster head and two stations are five hops from cluster head. The average station's location errors at different packet errors are shown in Figure 5-9. The station location errors increase sharply when increasing the packet errors from 5% to 20%. At 20% packet errors, the station location errors exceeds 10 mm in north component, 20 mm in east component and 30 mm in up component with 95% confidence interval. When further increase the packet errors, the percentage of data lost when transfer of stations five hops a way from cluster head is 83% and 92% when communication packet errors are 30% and 40% respectively. As a result, two stations five hops away from cluster do not have enough data to be processed. They will be removed from processed stations list. However, the stations location errors of the remaining stations in this setting are still higher than when packet errors are less than 30%. When the packet errors are 40%, the vertical component exceeds 100 mm.

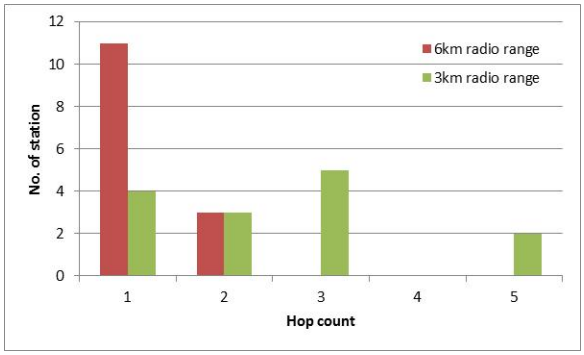

Figure 5-8 Number of hop count

In the second experiment, assuming the maximum radio range of 6 km could be archived without the need of relay stations or repeaters. In addition, the observation single-frequency GPS data is sampling at 30 s. Station TVST is selected as the cluster head to keep balance between the total numbers of hop count of the mesh network and minimal hop count from reference station to cluster head. Hop count distribution of stations in the network is shown in Figure 5-8. It can be seen that most stations including KAYT reference station are one hop away from cluster head and the other three stations are two hops

away from the cluster head. Stations location errors with respect to different packet errors are shown in Figure 5-10. The stations location errors increase almost linear when increasing the packet errors from 10% to 50%. It exceeds 60 mm in east and up component when packet errors are 50%. When comparing to the previous experiment, the stations location errors reduce more than 50% when increasing the radio range from 3 km to 6 km.

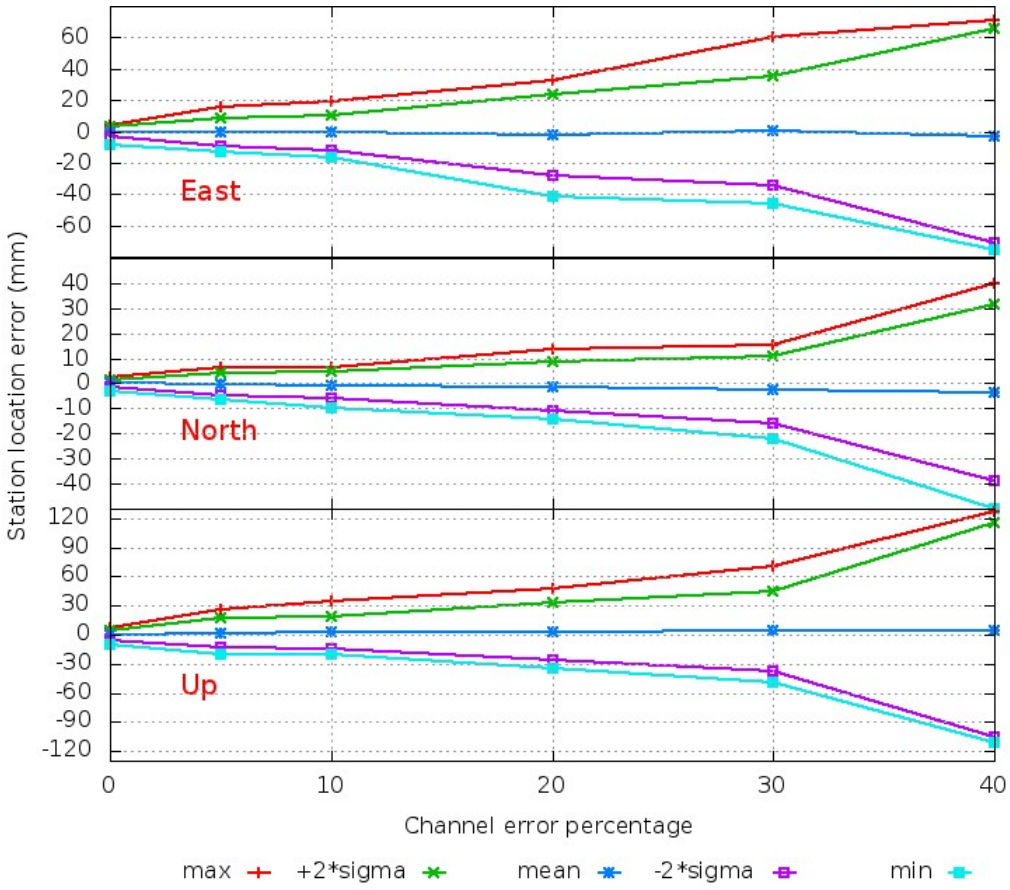

Figure 5-9 Stations location errors at 3 km radio range

The stations location errors at 3 km radio range are almost triple the station location errors at 6 km radio range when packet errors are 40%. In both experiments, the horizontal component errors are less than 15 mm if the packet errors are kept lower than 10%.

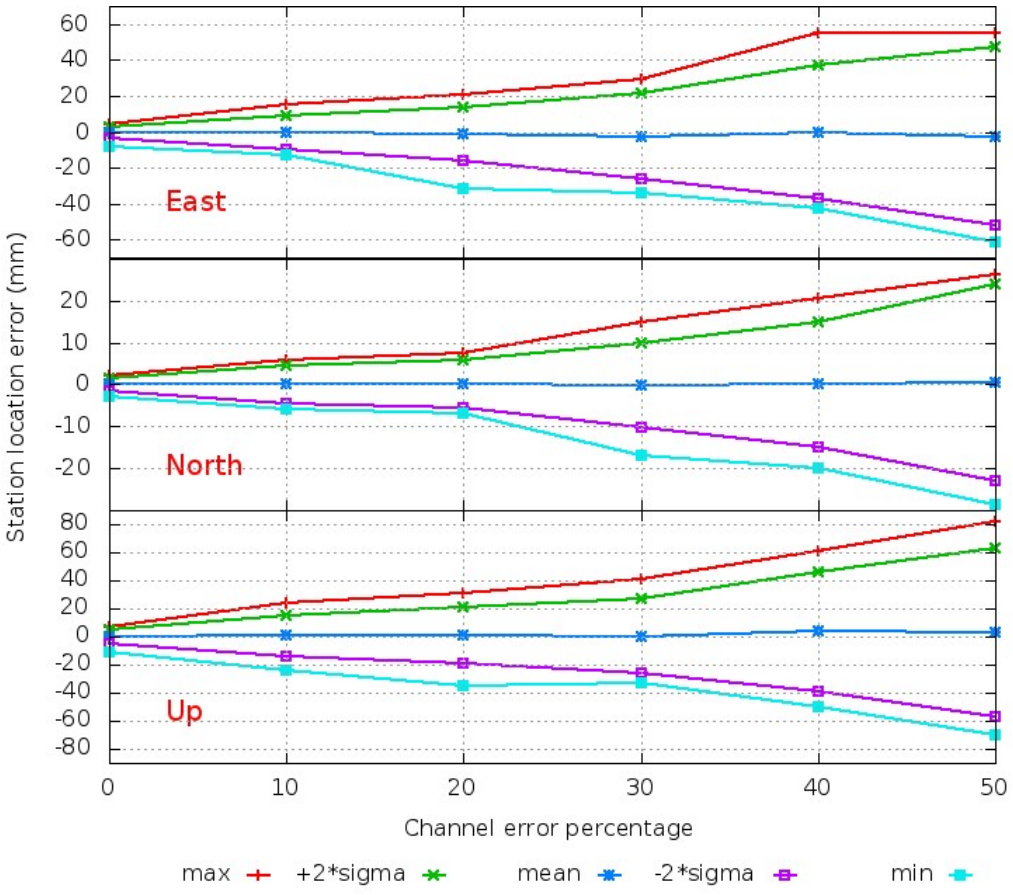

Figure 5-10 Stations location errors at 6 km radio range

5.6. Summary

The considerably high coordinate scatter in the east component of Taal's single-frequency data is a function of distance from the reference station, reflecting the high ionospheric gradient presented at low latitudes area. Regardless of the coordinate scatter, the proposed method could estimate stations location of single-frequency GPS station with the level of accuracy to estimate the deformation in all three components.

In-network distributed single-frequency GPS processing method is proposed with four main steps: dual-frequency station location estimation, reference station selection, GPS station clustering and cluster base GPS processing. Four network setups are studied to evaluate the proposed method in three main performance attributes: 1) number of up-link reduction, 2) stations location errors and 3) communication bandwidth. The results

show the proposed in-network single-frequency GPS method significantly reduces the number of long-range uplink required for GPS network. Furthermore, stations location errors are very sensitive to packet errors especially at short radio range when some stations in the network are more than two hops away from the cluster head. The bandwidth required for daily solution is supported by low power long-range radio module.

CHAPTER 6

PROOF OF CONCEPT DEPLOYMENT

In this part, the ongoing research of design, evaluate and deploy a proof-of-concept in-network single-frequency GPS processing system is presented.

6.1. System Design

The system design is a challenge task to keep it balance of computation power to transmit and processing raw GPS data in real-time, easy to deploy in a hostage environment and cost-effective.

6.1.1. Hardware design

The hardware modules are encapsulated in a small waterproof case with dimensions of 19 cm x 17 cm (Figure 6-1). The box contains a Gumstix Verdex Pro XL6P embedded processor module, a customized peripheral board, two low-cost single-frequency L1 Original Equipment Manufacturers (OEM) receivers, two RF modules and expansion connectors. The Gumstix module is selected instead of other processor modules and sensor network platforms such as Beagle boards, Libelium Waspmotes, Sun SPOT, and Crossbow motes; as it keeps balance between the computational powers required to process GPS raw data with real-time or scientific post-process software and power consumption of the whole system. Gumstix Verdex Pro XL6P board has a PXA270 processor with maximum speed of 600 MHz; it has 128 MB RAM, 32 MB Flash and an external SD card reader. Moreover, it has rich I/O interfaces including flexible connectors with 60-pins, 80-

pins and 24-pins, USB full speed (v1.1) host signal, 10 data bits of CIF signals, three UART, three NSSP and multiple GPIO interfaces.

The two low-cost L1 GPS receivers, an Ublox LEA-5T and an Ashtech AC12 are connected to the customized-peripheral board using UART and USB interface respectively for raw GPS data and Pulse-Per-Second (PPS) signal. These signals from two GPS receivers are connected to the GPIO pins of Gumstix board. The two GPS receivers are configured to raw data mode in order to provide raw GPS measurement and navigation information. Two RF modules comprise an XBee-PRO DigiMesh 900 and an XBee-PRO DigiMesh 2.4 to support mesh network connections among GPS stations with different range and bandwidth requirements. Mesh network is established between stations to broadcast raw GPS data, location information and adjustments to other stations. RF modules are connected to the customized peripheral board using UART interface.

Figure 6-1 Deployment box

The total construction cost of each low-cost GPS station (which includes GPSs, RFs, antennas, Gumstix CPU board and customized board) is about $700. With the same budget to acquire one scientific grade GPS station (typical $20K or more required for a scientific grade GPS station with a choke ring antenna [86]), a mesh network of low-cost GPS station with 10 to 20 stations could be constructed. It could be very meaningful in

study a small active tectonic or volcanic plate. Because the mesh network could be deployed in bigger area and it has higher redundancy in the network when comparing to single scientific grade GPS station.

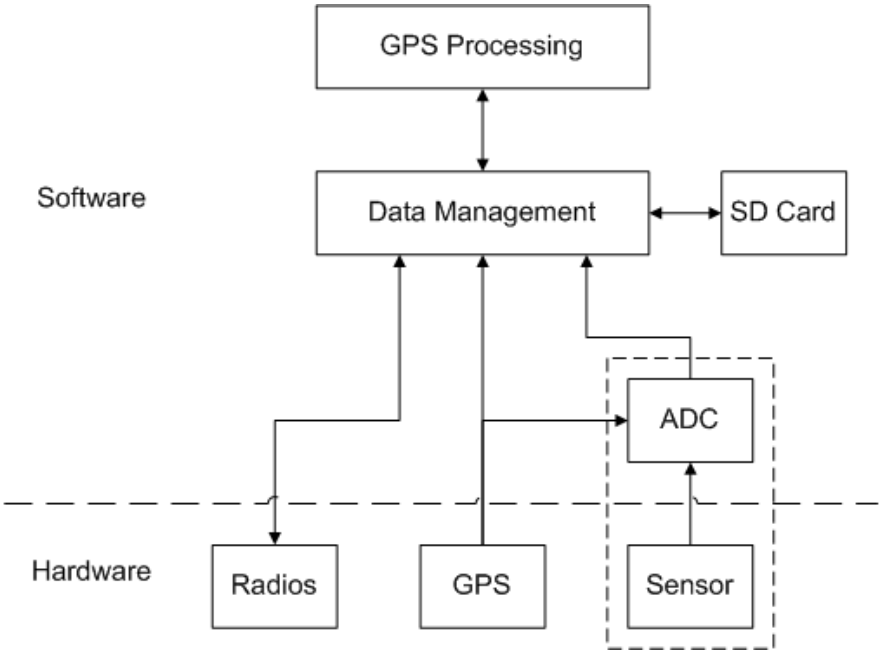

Figure 6-2 System design architecture

6.1.2. Software design

The Gumstix embedded processor board runs a customized version of Linux OS, the de factor operation system for most of GPS processing software. The Linux OS was selected to make use of both commercial and free open source software to download, convert and process GPS data. The tight decoupling integration of hardware and software stack is shown in Figure 6-2. An analog to digital converter with GPS time synchronization and an additional sensor signal aggregation capability are preserved for future usage (shown in dashed rectangle). The data management block is the main software component of the system. It controls the data manipulation of raw GPS data stream receiver and the GPS processing software at the local station as well as the stream of adjustment data received from other stations in the network. A modified version of GPSTk [87], an open source GPS processing software is used for processing GPS data stream.

6.1.3. Distributed GPS processing

Deformation monitoring using GPS is usually carried out by establishing and operating a local network of GPS receivers located on and around the deforming area. In order to reduce the cost of such a deformation monitoring system, single-frequency GPS receivers need to be used. It is assumed that the differential ionospheric and tropospheric delays between two receivers can be ignored if baseline lengths are kept below 10 km. It is the most common deployment setup when monitor a small active deformation site with a dense single-frequency GPS network.

The architecture of the proposed low-cost single-frequency GPS system could support real-time distributed GPS processing by sending raw GPS data from subset of the stations in the network to the remaining stations to process it in real-time. The selected sub-set will be considered as “fix reference stations” for the single-frequency GPS network. Fix reference could be selected by following characteristic: stations located far away from the remain station of the network, stations located at the less active frank of a volcano or near a dual-frequency GPS station with high accurate location. Location of stations in network could be estimated by using Double Difference (DD) phase base processing method with a modified version of GPSTk [87]. The GPS processing takes place at every station in the mesh network with stream of raw GPS data from reference stations and raw GPS data from the station itself. Final stations location or events detected could be relayed to centralized server without the need to send all high frequency GPS data outside the mesh network.

6.2. System Deployment and Processing Results

A small proof of concept deployment, its results and utilized mesh network setups will present in the following parts.

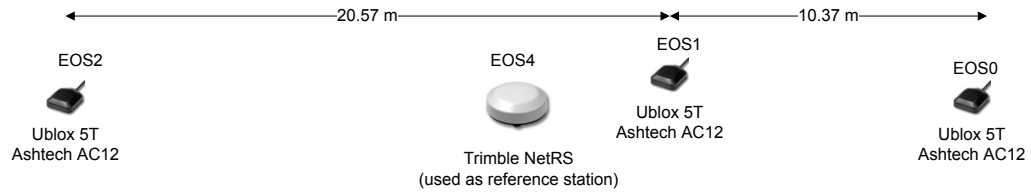

Figure 6-3 Proof of concept deployment topology

6.2.1. Proof of concept deployment

A proof of concept deployment is carried during the first two week of March 2011 with 3 low-cost GPS stations namely EOS0 to EOS2 with low profile antennas and a highly accurate Trimble NetRS dual-frequency scientific grade GPS receiver equipped with a choke ring antenna, EOS4 station (Figure 6-3). The Trimble station is used for reference and analytical purpose. The experimental devices are deployed at the roof top of a building at Nanyang Technological University with clear sky view. A mesh network connection is established between stations to exchange raw GPS data using DigiMesh firmware [88] of XBee PRO RF module.

6.2.2. Processing result

To compare estimated location of single-frequency GPS stations using different processing method, the location of single-frequency stations are estimated as follows steps.

1. The dual-frequency stations location are calculated using the most accuracy processing method which takes advantage of both L1 and L2 frequency and final satellite orbit and clock parameters.
2. Single-frequency GPS stations' location are estimated using Double Difference (DD) phase base processing method with reference stations location estimated in step 1.
3. Single-frequency stations location are estimated using different method without information about dual-frequency station location in step 1.

4. Processing error is calculated by subtract the estimated location in step 3 to the estimated locations in step 2 of the same single-frequency station, as in (6.1).

$$ProcessingError = P_{withoutReferenceStations} - P_{withReferenceStations} \quad (6.1)$$

In the proof of concept deployment, location of the dual-frequency reference station, EOS4, is estimated using both L1 and L2 frequencies. The Precise Point Positioning (PPP) processing method with final satellite orbit and clock product was used to process GPS raw data using GIPSY [49] software package at sampling rate 1s. Location of single-frequency GPS stations in network is estimated using Double Difference (DD) phase base processing method with EOS4 as reference station with estimated location just calculated above. This estimated location of single-frequency GPS stations is used to calculate position error of other processing methods, as in (1).

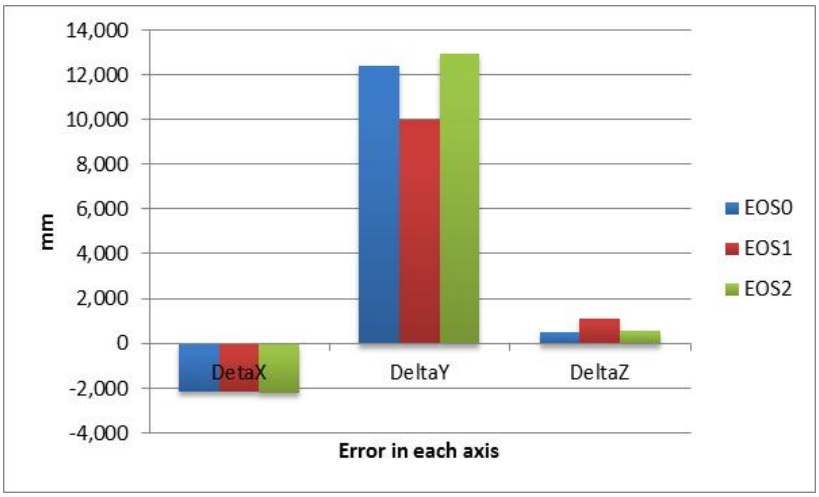

Figure 6-4 Single station processing error

Without mesh network single-frequency stations work independently, in this network setup only raw GPS data at each station is used to estimate location of that station. The result of real-time processing data using only single-frequency data is shown in Figure 6-4 using RAIM like processing method. The error is bigger than 10 m in Y axis and about 2 m for both X and Z axis. The magnitude of error is too big for real-time deformation detection.

With the mesh network, raw GPS data could be transmitted between GPS stations in the mesh network in real-time. Three processing strategies are used in which one of the single-frequency GPS station is fixed as reference station for other two stations in the network. The processing error is calculated as in (1) and the result is showed in Fig. 5. The processing error in Fig. 5 is smaller when compared to processing error in case of each single-frequency GPS station is processed independently in Fig. 4. The processing error in X, Y and Z axis are less than 3 mm.

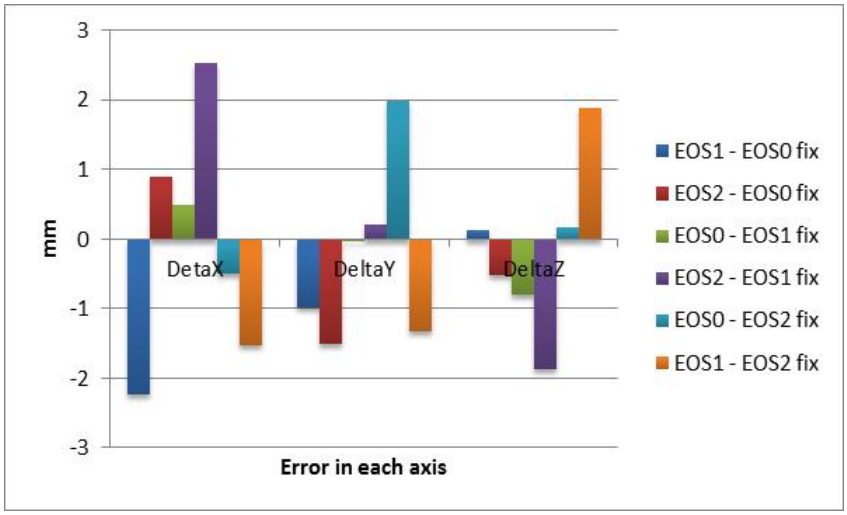

Figure 6-5 Collaboration processing error

6.2.3. Mesh network capability

Mesh networking allows GPS data from pre-define reference stations to be sent through several different GPS stations or hops to a final destination stations. In this deployment DigiMesh firmware [88], the default and supported firmware of Xbee-PRO DigiMesh product line, is used. This mesh firmware supports the self-healing, route discovery, peer-to-peer architecture, and selective acknowledgement attributes of mesh networking. The advantage of mesh network is in the event that one RF connection between nodes is lost (due to power-loss, environmental obstructions, etc.) critical GPS data can still reach its final GPS station due to the mesh networking capabilities embedded inside the XBee-PRO modules.

The transmission range and throughput written in datasheet of Xbee-PRO DigiMesh [88] radio is presented in Table 6-1 and Table 6-2 respectively.

Specification	Xbee-PRO DigiMesh	
	900 MHz	***2.4 GHz***
Indoor/Urban Range	Up to 140m	Up to 90m
Outdoor RF line-of-sight Range	Up to 3km with 2.1dB dipole	1500m

Table 6-1 XBee-PRO DigiMesh transmission range

Configuration	Xbee-PRO DigiMesh	
	900 MHz	***2.4 GHz***
1 hop, Encription Disabled	87.1 kbps	27.0 kbps
3 hop, Encription Disabled	33.9 kbps	10.9 kbps
6 hop, Encription Disabled	17.0 kbps	5.78 kbps
1 hop, Encription Enabled	78.9 kbps	20.5 kbps
3 hop, Encription Enabled	32.8 kbps	9.81 kbps
6 hop, Encription Enabled	16.5 kbps	4.7 kbps

Table 6-2 Xbee-PRO DigiMesh throughput

During deployment campaign on the first two week of March 2011, the maximum size of single-frequency GPS data per day is about 50MB with average 10 satellites is see in the sky. As the result, the maximum data could generate from single-frequency GPS station about 100MB per day when more satellites are seen by GPS stations. The minimum required bandwidth to transmit that amount of GPS data in real-time is bigger than 9.5kbps. In un-encryption mode, the DigiMesh could support up to six hops when using 900MHz radio and up to three hops when using 2.4 GHz radio. With that number of hops, the propose WMN could cover an area with diameter up to 10 km which is required for deformation monitoring with single-frequency GPS network in an active deformation site.

6.3. Conclusions

This section presents an ongoing study on the use of wireless mesh network supported low-cost in-network distributed GPS processing. The results show that this method significantly reduces the station location errors and makes use of the computational capa-

bility of station in-network to process GPS data. The developed hardware and software system could cover an area up to 10 km in diameter, which is adequate to cover an active deformation-monitoring site. A detail analysis of this network with a larger coverage and with real deployment in the crater of active volcano should be conducted to verify the processing capability and system performance under challenging environment.

However, a full system deployment is nearly impossible due to two reasons. First, the 900 MHz radio frequency modules are used in this study as the long-range light-of-sight modem. This frequency is banned in Singapore and most of other Asian countries because it could interference with GSM signal. Moreover, it could be extremely hard to test that kind of long-range radio in Singapore; it requires light-of-sight clearance between stations from 5 km up to 90 km. In the very early state on this research, others member of the author's team had a chance to test the radio in Indonesia with the support of Earth Observatory of Singapore (EOS) and EOS's local collaborator institutions. Second, when the author finished the development of the experiment system present in the final part of this thesis, he doesn't have the support from EOS for the system deployment. It is almost impossible to test the system without the support from local partner in Indonesia or elsewhere and without finance support from EOS.

CHAPTER 7

SUMMARY AND CONCLUSIONS

7.1. Summary

Ground deformation activities of a volcanic or tectonic plate are considered as an early signs of forthcoming eruptive activities. GPS with its spatial and temporal properties is an ideal method for detecting and monitoring such deformation events. In this thesis, mesh networks are studied to minimize operation cost of existing dual-frequency GPS array and reduce stations location errors in in-network single-frequency GPS processing.

In cGPS arrays utilizing satellite or long-range LoS wireless communications, each GPS station in the cGPS array will periodically measure the tectonic and/or meteorological data and store the measured data locally. This observed GPS data is sent to a data server through a dedicated uplink from the stations at various update intervals. In this thesis, mesh network is studied to reduce the operational expenditure by reducing number of uplinks and the amount of data transmitted via those links. Moreover, single-frequency GPS processing method that utilized wireless mesh network has been proposed, in order to enhance the existing deployed continuous low-cost single-frequency GPS deformation monitoring and hazard mitigation system. Although this thesis mainly focuses on tectonic and volcanic deformation monitoring, the proposed methodology could be used for a variety of structure monitoring or hazard mitigation applications, such as for landslides, open-cut mines, dams,

bridges, high-rise buildings. The contributions of this thesis are encapsulated in Figure 7-1. They will briefly described in following sections.

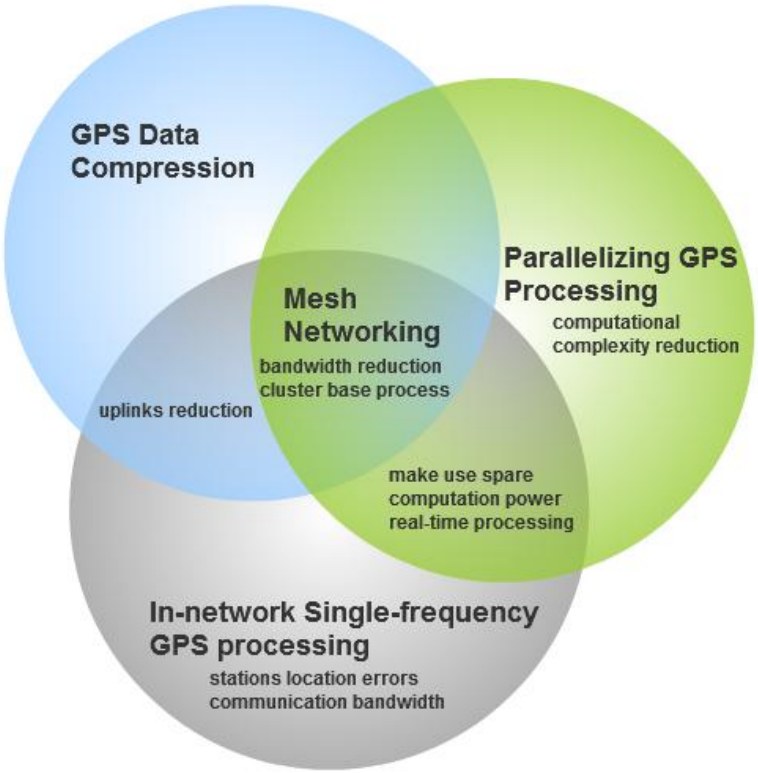

Figure 7-1 Contribution of the study

7.1.1. Mesh networking for GPS data compression

Modifications of the Sumatran cGPS array are proposed to utilize wireless mesh network in order to reduce the expenditure of satellite communication subscription of the cGPS array by removing correlation observation information and reducing the number of costly satellite uplinks required.

Wireless mesh networks can be established using long-range radios. These radios provide a point-to-point line-of-sight wireless communication link. Multi-hop communications can be utilized by deploying relay stations to overcome obstructions or long distances. Depending on the budget, geographical, power restriction or latency considerations, the

number of hops and the radio range supported may be limited. Clusters of GPS stations will be formed and a cluster-head would be selected for each cluster. Each cluster-head will have satellite communication capabilities and will be responsible for collecting all the observation data from the GPS stations within the cluster and transmitting them to the remote centralized data server. Mesh network greatly reduces the number of satellite links needed by the GPS network, as each cluster requires a minimum of only one satellite uplink. With SuGAr GPS data, assuming the maximum range of 90 km could be achieved with the absence of relay stations or repeaters. Thirteen satellite links will have to be maintained for 24 GPS stations of SuGAr array. However, given a maximum radio range of 250 km, all Sumatran's GPS stations are grouped into one cluster using only one uplink.

Each cluster-head will compress the observation data from all GPS stations within the cluster using the LZMA algorithm prior to transmit via the satellite link. Compared to the existing SuGAr deployment where each GPS station transmits the observation data independently, the use of mesh networking allows larger datasets to be formed through the aggregation of observation data from each GPS station within a cluster. Given that the compression ratio of SuGAr GPS data will increase when increasing the dataset size to be compressed by adding more stations to the WMN, the number of data transmitted via the satellite will be significantly reduced. Cluster base compression method reduces more than 70% of daily data upload when comparing to uncompressed processing method. The efficiency of this method will increase considerably to 83% when increase GPS data upload frequency from daily to two minutely as the amount of upload data will increase.

Wireless mesh networks are proposed by mean of long-range radios and data aggregation is performed to enable cluster-based compression. Using the actual data captured from the Sumatran cGPS array in the evaluation and analysis processing, it is concluded

that the proposed use of mesh networking not only reduces the number of costly satellite uplinks required to one uplink, it also significantly reduces the total amount of data transferred through these links up to 83% at two minute upload frequency.

7.1.2. Mesh network for parallelizing the computation of GPS processing

In-situ parallel and distributed processing of GPS corrections could be made possible using mesh networking. The observation data from adjacent GPS stations can be grouped together and processed in a hierarchical fashion. Compared to the conventional methods of sequential GPS processing, the computational complexity and computation time of parallel and distributed GPS processing with various schemes decrease significantly. By sharing data within the mesh network, it is possible for in-network processing to be performed for GPS corrections using the processing capability of embedded system at each GPS station. This allows early-warning applications to be developed without the need for costly data transmission to a remote centralized processing facility.

By reducing the computational complexity, the proposed computation model promises to make use of small, low-cost embedded system which already available or could easily be deployed in cGPS network, such as routers or station controllers. The dedicated wireless mesh network connection between stations is utilized to transmit and collaborative process GPS data in real-time or near real-time fashion.

7.1.3. In-network single-frequency GPS processing for volcano monitoring

Active volcano deformation monitoring using GPS could be possible out by establishing and operating a network of continuous GPS receivers located on and around the deforming area. In order to reduce the expenditure of constructing and maintaining the network as well as increasing coverage area of such a deformation monitoring system, sin-

gle-frequency GPS receivers are preferred over dual-frequency GPS receivers. With single-frequency GPS monitoring system, the baseline lengths are kept less than 10 kilometers. In such a small network, the tropospheric and ionospheric delays between two receivers are nearly zero. Furthermore, orbit bias over such short distances can also be ignored.

The proposed distributed GPS processing method is designed for a small coverage and mix-mode GPS network with WMN connection between stations. The WMN is utilized to exchange raw GPS data, estimated corrections as well as processing results. These types of mix-mode GPS network include single-frequency and dual-frequency GPS receivers deployment around an active volcanic or tectonic plate. Four proposed steps of distributed GPS processing are described including: dual-frequency station location estimation, reference station selection, GPS station clustering and cluster base GPS processing.

The processing results of Taal GPS data show that the considerably high coordinate scatter in the east component of Taal's single-frequency data is a function of distance from the reference station, reflecting the high ionospheric gradient presented at low latitudes area. Regardless of the coordinate scatter, the stations location of satiation with single-frequency GPS receiver is estimated with the level of accuracy sufficient to estimate the deformation in all three components.

Four network setups are studied to evaluate the proposed in-network single-frequency GPS processing method. The results show the proposed method significantly reduces the number of long-range uplink required for the whole GPS array. Furthermore, stations location errors are very sensitive to channel error especially at sort radio range when some stations in the network are more than two hops away from the cluster head. The bandwidth required for daily solution is well supported by low power long-range radio modules which is used in this study.

7.2. The Limitation of The Proposed Wireless Mesh Network

The proposed wireless mesh network in chapter 5 is using point-to-point long-range wireless connection between GPS stations. Due to the multiple hop transmission and the lack of redundancy upload link, a single station failure may pose a serious problem to the network. The wireless mesh network could be partitioned into two sub-networks with no communications between them.

The site construction and maintenance of the line-of-sight link between stations could be a challenge because stations are usually located at remote area or hazardous environment near volcanic or tectonic plates which may not be accessed easily.

7.3. Suggestion and Recommendation for Future Research

Wireless mesh network (WMN) connections between GPS stations empower them the ability to share information and adjustments estimation in real-time. In the future, more research will be conducted to study the collaborative GPS processing within a mesh network of GPS stations. The suggestion of future research is to exploit mesh networking with three main objectives: communication bandwidth reduction, environment awareness processing, and real-time events monitoring.

The data compression algorithm presents in this thesis utilizing a PC based data compression (7Zip) algorithm. It does not take into account GPS data correlation and power limitation of remote GPS stations. Nevertheless, data correlation exists between consecutive GPS measurements (epochs) at the same station or between epochs at different stations which share common satellites. Exploration of data correlation could decrease transmission data and reduce power consumption required for up loading data to centralized processing facility. The new compression algorithm has to take into account battery ca-

pacity or energy level at the node during the processing time, such as the work presented by K. C. Barr for energy awareness data compress [89]. Another direction is to explore lossy data compression algorithms which is successfully used in WMN deployments [90], as demonstrated in the micro climate monitoring project. Lossy compression data could be used as long as it kept the estimated GPS stations location error less than a predefined thread hold, which could be determined by level of accuracy required by each network and calibration adjustments error.

Distributed GPS processing reduces computation complexity and computation time. It enables embedded device to processing GPS data in real-time. Moreover, event detection algorithm using single GPS station may fail to detect events that cause by noisy data or human made events. The collaboration GPS processing to detect seismic or tectonic events is efficiently deployed for networks monitoring volcanoes [72, 73]. It adjusts sampling rate when the event happens, taking into account the event type and memory capacity of the nodes in network.

The initial results of a proof of concept deployment of an in-network single-frequency GPS processing system for volcano monitoring are presented in chapter 6. The results show that this method significantly reduces the station location errors and makes use of the computational capability of station in the network to process GPS data. The larger deployment should be study in the future with a larger coverage network and with actual deployment in the crater of active volcano would be studied in the future to verify the processing capability and system performance under hazardous environment.

The challenges of real-time GPS processing method using low-cost GPS receivers and WMN is that the GPS processing algorithms in the literature are mostly designed for post processing which make use of a centralized PC/server base system facility. Modifica-

tion of current GPS processing algorithms or development of new algorithms for real-time processing using localized embedded systems and the WMN have to be investigated. These algorithms should take advance of addition sensors will be deployed at single-frequency GPS stations to support a fast and early warning events detection mechanism.

List of Publications

1) H.-H. Tran and K.-J. Wong, "Mesh Networking for Seismic Monitoring - The Sumatran cGPS Array Case Study," in Wireless Communications and Networking Conference, 2009. WCNC 2009. IEEE, 2009, pp. 1-6.

2) H.-H. Tran and K.-J. Wong, "Usage of Mesh Networking in a Continuous-Global Positioning System Array for Tectonic Monitoring," in *Communication and Networking*, ed: SCIYO, 2010.

3) H.-H. Tran and K.-J. Wong, "Wireless Mesh Networking for In-Network Processing of Low-cost GPS Devices," in The 7th International Conference on Wireless Communications, Networking and Mobile Computing, WiCOM2011, Wuhan, China, 2011, pp. 1-4.

4) H.-H. Tran and K.-J. Wong, "Real-time In-network Single-frequency GPS Processing for Deformation Monitoring," in Wireless Communications and Networking Conference, 2012. WCNC 2012. IEEE, Paris, France, 2012, pp. 3305-3309.

REFERENCES

[1] S. Stein and E. A. Okal, "Seismology: Speed and size of the Sumatra earthquake," *Nature,* vol. 434, pp. 581-582, 2005.

[2] S. Ni, H. Kanamori, and D. Helmberger, "Seismology: Energy radiation from the Sumatra earthquake," *Nature,* vol. 434, pp. 582-582, 2005.

[3] C. J. Ammon, C. Ji, H.-K. Thio, D. Robinson, S. Ni, V. Hjorleifsdottir, *et al.*, "Rupture Process of the 2004 Sumatra-Andaman Earthquake," *Science,* vol. 308, pp. 1133-1139, May 20 2005.

[4] T. Lay, H. Kanamori, C. J. Ammon, M. Nettles, S. N. Ward, R. C. Aster, *et al.*, "The Great Sumatra-Andaman Earthquake of 26 December 2004," *Science,* vol. 308, pp. 1127-1133, May 20 2005.

[5] K. Sieh, D. H. Natawidjaja, A. J. Meltzner, C.-C. Shen, H. Cheng, K.-S. Li, *et al.*, "Earthquake Supercycles Inferred from Sea-Level Changes Recorded in the Corals of West Sumatra," *Science,* vol. 322, pp. 1674-1678, December 12 2008.

[6] S. V. Sobolev, A. Y. Babeyko, R. Wang, A. Hoechner, R. Galas, M. Rothacher, *et al.*, "Tsunami early warning using GPS-Shield arrays," *J. Geophys. Res.,* vol. 112, pp. 1-18, 2007.

[7] (2009, December). *The Sumatran Plate Boundary Project*. Available: http://www.tectonics.caltech.edu/sumatra/

[8] (2009, December). *Andean Subduction Project*. Available: http://www.tectonics.caltech.edu/andes/

[9] (2009, December). *Himalayan Tectonics and Seismicity*. Available: http://www.gps.caltech.edu/~avouac/research.html

[10] N. Patterson, K. Gledhill, and M. Chadwick, "New Zealand National Seismograph Network Report for the Federation of Digital Seismograph Networks Meeting, 2007," 2007 FDSN Meeting, Perugia, Italy8-11 July 2007.

[11] T. Sagiya, "A decade of GEONET: 1994-2003-The continuous GPS observation in Japan and its impact on earthquake studies-," *Earth, Planets Space,* vol. 56, pp. XXIX-XLI, 2004.

[12] K. W. Hudnut, Y. Bock, J. E. Galetzka, F. H. Webb, and W. H. Young, "The Southern California Integrated GPS Network (SCIGN)," *10th International Symposium on Crustal Deformation Measurement,* pp. 129-148, March 19-22 2001.

[13] B. A. Bartel, M. W. Hamburger, C. M. Meertens, A. R. Lowry, and E. Corpuz, "Dynamics of active magmatic and hydrothermal systems at Taal Volcano, Philippines, from continuous GPS measurements," *J. Geophys. Res.,* vol. 108, p. 2475, 2003.

[14] V. Janssen, C. Roberts, C. Rizos, and H. Z. Abidin, "Low-cost GPS-based volcano deformation monitoring at Mt. Papandayan, Indonesia," *Journal of Volcanology & Geothermal Res.,* vol. 115, pp. 139-151, 2002.

[15] H. Allen, S. Igor, L. Martin, N. Vinayak, G. Richard, D. Paul*, et al.*, "WiLSoN: The Wirelessly Linked Seismological Network and Its Application in the Middle American Subduction Experiment," *Seismological Research Letters,* vol. 79, pp. 438-443, 2008.

[16] G. Beutler, A. Moore, and I. Mueller, "The international global navigation satellite systems service (IGS): development and achievements," *Journal of Geodesy,* vol. 83, pp. 297-307, 2009.

[17] J. M. Dow, R. E. Neilan, and G. Gendt, "The International GPS Service: Celebrating the 10th anniversary and looking to the next decade," *Advances in Space Research,* vol. 36, pp. 320-326, 2005.

[18] J. Kouba. (2009, via IGS. http://acc.igs.org/UsingIGSProductsVer21.pdf. Accessed 31 August 2009). *A guide to using international GNSS service (IGS) products*.

[19] A. Leick, *GPS satellite surveying*, 3rd ed. Hoboken, NJ: John Wiley, 2004.

[20] W. Gurtner and L. Estey. (2007). *RINEX The Receiver Independent Exchange Format Version 3.00*. Available: available from ftp://igscb.jpl.nasa.gov/igscb/data/format/rinex300.pdf

[21] Y. Hatanaka, "A RINEX Compression Format and Tools," in *Proceedings of ION GPS-96*, 1996, pp. 177-183.

[22] S. Doong, "A closed-form formula for GPS GDOP computation," *GPS Solutions,* vol. 13, pp. 183-190, 2009.

[23] D.-J. Jwo and C.-C. Lai, "Neural network-based GPS GDOP approximation and classification," *GPS Solutions,* vol. 11, pp. 51-60, 2007.

[24] S. Bancroft, "An Algebraic Solution of the GPS Equations," *Aerospace and Electronic Systems, IEEE Transactions on,* vol. AES-21, pp. 56-59, 1985.

[25] E. W. Grafarend and J. Shan, "GPS Solutions: Closed Forms, Critical and Special Configurations of P4P," *GPS Solutions,* vol. 5, pp. 29-41, 2002.

[26] J. Zumberge, M. Heflin, D. Jefferson, M. Watkins, and F. Webb, "Precise point positioning for the efficient and robust analysis of GPS data from large networks," *J. Geophys. Res.,* vol. 102, pp. 5005-5017, 1997.

[27] J. Kouba and P. Héroux, "Precise Point Positioning Using IGS Orbit and Clock Products," *GPS Solutions,* vol. 5, pp. 12-28, 2001.

[28] Y. Gao and K. Chen, "Development of a Real-Time Single-Frequency Precise Point Positioning System and Test Results," in *ION GNSS 2006*, Fort Worth, TX, USA, 2006.

[29] A. Le and C. Tiberius, "Single-frequency precise point positioning with optimal filtering," *GPS Solutions,* vol. 11, pp. 61-69, 2007.

[30] A. E. Niell, "Global mapping functions for the atmosphere delay at radio wavelengths," *J. Geophys. Res.,* vol. 101, 1996.

[31] J. Saastamoinen, "Atmospheric Correction for Troposphere and Stratosphere in Radio Ranging of Satellites," *Geophysics Monograph Series,* vol. 15, 1972.

[32] V. B. Mendes and R. B. Langley, "Tropospheric Zenith Delay Prediction Accuracy for Airborne GPS High-Precision Positioning," in *The Institute of Navigation 54th Annual Meeting*, Denver, CO, U.S.A, 1998.

[33] S. Bisnath and Y. Gao, "Current State of Precise Point Positioning and Future Prospects and Limitations," ed, 2008, pp. 615-623.

[34] R. J. Muellerschoen, W. I. Bertiger, M. Lough, D. Stowers, and D. Dong, "An Internet-Based Dual-Frequency Global Differential GPS System," in *IAIN World Congress*, San Diego, CA, 2000.

[35] M. O. Kechine, C. C. J. M. Tiberius, and H. Marel, "An experimental performance analysis of real-time kinematic positioning with NASA's Internet-Based Global Differential GPS," *GPS Solutions,* vol. 8, pp. 9-22, 2004.

[36] M. O. Kechine, C. C. J. M. Tiberius, and H. v. d. Marel, "Real-time Kinematic Positioning with NASA's Global Differential GPS System," presented at the GNSS Conference, St. Petersburg, Russia, 2004.

[37] T. Sharpe, R. Hatch, and F. Nelson, "StarFire and Real-Time GIPSY: A Global High-Accuracy Differential GPS System," presented at the 4th International Symposium on GPS/GNSS, Wuhan University, China, 2002.

[38] H. Yousif and A. El-Rabbany, "Assessment of Several Interpolation Methods for Precise GPS Orbit," *The Journal of Navigation,* vol. 60, pp. 443-455, 2007.

[39] H. Bock, R. Dach, A. Jäggi, and G. Beutler, "High-rate GPS clock corrections from CODE: support of 1 Hz applications," *Journal of Geodesy,* vol. 83, pp. 1083-1094, 2009.

[40] B. Hofmann-Wellenhof, H. Lichtenegger, and J. Collins, *Global Positioning System : theory and practice*, 4th, rev. ed. Wien ; New York: Springer-Verlag, 1997.

[41] B. Zebhauser, H.-J. Euler, R. Keenan, and G. Wübbena, "A Novel Approach for the Use of Information from Reference Station Networks Conforming to RTCM V2.3 and Future V3.0," in *ION NTM 2002*, San Diego, California, 2002.

[42] G. Lachapelle, P. Alves, L. P. Fortes, M. E. Cannon, and B. Townsend, "DGPS RTK Positioning Using a Reference Network," in *13th International Technical Meeting of the Satellite Division of the Institute of Navigation (ION GPS 2000)*, Salt Lake City, UT, 2000, pp. 1165 - 1171.

[43] U. Vollath, A. Buecherl, H. Landau, C. Pagels, and B. Wagner, "Multi-Base RTK Positioning Using Virtual Reference Stations," in *13th International Technical Meeting of the Satellite Division of the Institute of Navigation (ION GPS 2000)*, Salt Lake City, UT, 2000, pp. 123 - 131.

[44] J. F. Raquet, "Development of a Method for Kinematic GPS Carrier-Phase Ambiguity Resolution Using Multiple Reference Receivers," PhD, Geomatics Engineering, The University of Calgary, Alberta, Canada, 1998.

[45] J. F. Raquet and G. Lachapelle, "Development and Testing of a Kinematic Carrier-Phase Ambiguity Resolution Method Using a Reference Receiver Network," *Navigation,* vol. 46, pp. 283-295, 2000.

[46] W. I. Bertiger, Y. E. Bar-Sever, B. J. Haines, B. A. Lijima, S. M. Lichten, U. J. Lindqwister*, et al.*, "A Real-Time Wide Area Differential GPS System," *invited Contribution to Institute of Navigation "Red Books," Global Positioning System: Papers Published in Navigation,* vol. IV, 1999.

[47] R. Dach, U. Hugentobler, P. Fridez, and M. Meindl, *Bernese GPS Software Version 5.0*. Astronomical Institute, University of Bern, 2007.

[48] T. A. Herring, R. W. King, and S. C. McClusky, "GAMIT reference manual - GPS Analysis at MIT," ed: Departement of Earth, Atmospheric, and Planetary Sciences, MIT, 2008.

[49] S. M. Lichten, Y. E. Bar-Sever, E. I. Bertiger, M. Heflin, K Hurst, R.J. Muellerschoen*, et al.*, "GIPSY-OASIS II: A High Precision GPS Data Processing System and general Satellite Orbit Analysis Tool," in *Jet Propulsion Laboratory*, ed. California Institute of Technology, Pasadena, CA., 1996.

[50] Brian Tolman, R. B. Harris, T. Gaussiran, D. Munton, J. Little, R. Mach*, et al.*, "The GPS Toolkit -- Open Source GPS Software," in *The 17th International Technical Meeting of the Satellite Division of the Institute of Navigation (ION GNSS 2004)*, Long Beach, California, 2004.

[51] D. Salazar, S.-S. J., and M. Hernandez-Pajares, "Phase-based GNSS data processing (PPP) with the GPSTk," in *The 8th geomatic week*, Barcelona. Spain 2009.

[52] A. O. Konca, J.-P. Avouac, A. Sladen, A. J. Meltzner, K. Sieh, P. Fang, *et al.*, "Partial rupture of a locked patch of the Sumatra megathrust during the 2007 earthquake sequence," *Nature,* vol. 456, pp. 631-635, 2008.

[53] Z. Li, J.-P. Muller, P. Cross, and E. J. Fielding, "Interferometric synthetic aperture radar (InSAR) atmospheric correction: GPS, Moderate Resolution Imaging Spectroradiometer (MODIS), and InSAR integration," *J. Geophys. Res.,* vol. 110, 2005.

[54] P. Segall and J. L. Davis, "GPS applications for geodynamics and earthquake studies," *Annual Review of Earth and Planetary Sciences,* vol. 25, pp. 301-336, May 1997.

[55] A. Yamagiwa, Y. Hatanaka, T. Yutsudo, and B. Miyahara, "Real-time capability of GEONET system and its application to crust monitoring," *Bulletin of the Geographical Survey Institute,* vol. 53, March 2006.

[56] (2009, December). *Earth Observatory of Singapore*. Available: http://www.earthobservatory.sg/

[57] C. M. Meertens, J. Braun, D. Mencin, C. Conquest, and L. Estey, "Development of a low cost single-frequency GPS system for volcano deformation monitoring," presented at the 1999 UNAVCO Volcano Geodesy Workshop, Jackson, Wyo., 1999.

[58] P. Cervelli, P. Segall, F. Amelung, H. Garbeil, C. Meertens, S. Owen, *et al.*, "The 12 September 1999 Upper East Rift Zone dike intrusion at Kilauea Volcano, Hawaii," *J. Geophys. Res.,* vol. 107, p. 2150, 2002.

[59] C. Rizos, S. Han, C. Roberts, X. Han, H. Z. Abidin, O. K. Suganda, *et al.*, "Continuously Operating GPS-Based Volcano Deformation Monitoring in Indonesia: The Technical and Logistical Challenges," in *IAG General Assembly*, Birmingham, UK, 2000, pp. 361-366.

[60] C. Roberts, C. Seynat, C. Rizos, and G. Hooper, "Low-Cost Deformation Measurement System for Volcano Monitoring," in *3rd FIG Regional Conference*, Jakarta, Indonesia, 2004.

[61] V. Janssen and C. Rizos, "Mixed-mode GPS deformation monitoring — A cost-effective and accurate alternative?," in *A Window on the Future of Geodesy*. vol. 128, F. Sansò, Ed., ed: Springer Berlin Heidelberg, 2005, pp. 533-537.

[62] (2011). *Movement Monitoring System*. Available: http://www.geodev.ch

[63] T. Iwabuchi, J. Johnson, S. Cummins, C. Rocken, Y. Iotake, and M. Kanzaki, "Deformation Monitoring with Single Frequency L1 Receivers," in *Proceedings of the 21st International Technical Meeting of the Satellite Division of the Institute of Navigation (ION GNSS 2008)*, Savannah, GA, 2008, pp. 3000-3008.

[64] I. F. Akyildiz and X. Wang, *Wireless mesh networks*: Chichester, U.K. : Wiley, 2009.

[65] G. Held, *Wireless mesh networks*: Boca Raton, FL : Auerbach Publications, 2005.

[66] R. Szewczyk, A. Mainwaring, J. Polastre, J. Anderson, and D. Culler, "An analysis of a large scale habitat monitoring application," presented at the Proceedings of the 2nd international conference on Embedded networked sensor systems, Baltimore, MD, USA, 2004.

[67] T. Gilman, P. Joseph, S. Robert, C. David, T. Neil, T. Kevin*, et al.*, "A macroscope in the redwoods," presented at the Proceedings of the 3rd international conference on Embedded networked sensor systems, San Diego, California, USA, 2005.

[68] K. Lakshman, A. Robert, B. Phil, C. Jasmeet, F. Mick, K. Nandakishore*, et al.*, "Design and deployment of industrial sensor networks: experiences from a semiconductor plant and the north sea," presented at the Proceedings of the 3rd international conference on Embedded networked sensor systems, San Diego, California, USA, 2005.

[69] I. Stoianov, L. Lachman, A. J. Whittle, S. Madden, and R. Kling, "Sensor networks for monitoring water supply and sewer systems, Lessons from Boston," *Proc. 8th Intl. Water Distribution Systems Analysis Symposium, (WDSA2006),* 2006.

[70] S. Kim, S. Pakzad, D. Culler, J. Demmel, G. Fenves, S. Glaser*, et al.*, "Health monitoring of civil infrastructures using wireless sensor networks," presented at the Proceedings of the 6th international conference on Information processing in sensor networks, Cambridge, Massachusetts, USA, 2007.

[71] G. Werner-Allen, J. Johnson, M. Ruiz, J. Lees, and M. Welsh, "Monitoring Volcanic Eruptions with a Wireless Sensor Network," in *Second European Workshop on Wireless Sensor Networks (EWSN'05)*, Istanbul, Turkey, 2005.

[72] G. Werner-Allen, K. Lorincz, M. Ruiz, O. Marcillo, J. Johnson, J. Lees*, et al.*, "Deploying a wireless sensor network on an active volcano," *Internet Computing, IEEE,* vol. 10, pp. 18-25, 2006.

[73] G. Werner-Allen, L. Konrad, J. Jeff, L. Jonathan, and W. Matt, "Fidelity and yield in a volcano monitoring sensor network," presented at the Proceedings of the 7th symposium on Operating systems design and implementation, Seattle, Washington, 2006.

[74] I. Stubailo, M. Lukac, M. Mayernik, E. Foote, R. Guy, P. Davis*, et al.*, "Subduction Zone Seismic Experiment in Peru: Results From a Wireless Seismic Network," *Center for Embedded Network Sensing. Posters,* p. 423, May 12 2009.

[75] M. Lukac, V. Naik, I. Stubailo, A. Husker, and D. Estrin, "In Vivo Characterization of a Wide area 802.11b Wireless Seismic Array," CENS Technical Report 2007.

[76] H.-H. Tran and K.-J. Wong, "Mesh Networking for Seismic Monitoring - The Sumatran cGPS Array Case Study," in *Wireless Communications and Networking Conference, 2009. WCNC 2009. IEEE*, Budapest, Hungary, 2009, pp. 1-6.

[77] W. Gurtner and G. Mader, "Receiver Independent Exchange Format Version 2," *GPS Bulletin,* vol. 3, pp. 1-8, 1990.

[78] Y. Hatanaka, "A Compression Format and Tools for GNSS Observation Data," *Bulletin of the Geographical Survey Institute,* vol. 55, March 2008.

[79] (2008). *FreeWave*. Available: http://www.freewave.com/

[80] J. Ziv and A. Lempel, "A Universal Algorithm for Sequential Data Compression," *IEEE Transactions on Information Theory,* vol. 23, pp. 337 - 343, May 1977.

[81] (2008). *SuGAr RINEX data at SOPAC*. Available: http://sopac.ucsd.edu/projects/sugar.html

[82] S.-i. Miyazaki, "Construction of GSI's Nationwide GPS Array," *Proceedings of the Joint Meeting of the U.S.-Japan Cooperative Program in Natural Resources Panel on Wind and Seismic Effects,* vol. 31, pp. 518-528, 1999.

[83] E. Serpelloni, G. Casula, A. Galvani, M. Anzidei, and P. Baldi, "Data analysis of permanent GPS networks in Italy and surrounding regions: application of a distributed processing approach," *Annals of Geophysics,* vol. 49, pp. 897-928, Aug-Oct 2006.

[84] C. Rizos, *Principles and Practice of GPS Surveying, Monograph 17*. Sydney, Australia: School of Geomatic Engineering, The University of New South Wales, 1997.

[85] (2012). *UNAVCO GPS Data*. Available: http://facility.unavco.org/data/dai2/app/dai2.html

[86] S. Wen-Zhan, H. Renjie, X. Mingsen, B. A. Shirazi, and R. LaHusen, "Design and Deployment of Sensor Network for Real-Time High-Fidelity Volcano Monitoring," *Parallel and Distributed Systems, IEEE Transactions on,* vol. 21, pp. 1658-1674, 2010.

[87] T. L. Gaussiran, E. Hagen, R. B. Harris, C. Kieschnick, J. C. Little, R. G. Mach, *et al.*, "The GPSTk: GLONASS, RINEX Version 3.00 and More," in *The 22nd International Technical Meeting of the Satellite Division of the Institute of Navigation (ION GNSS 2009)*, Savannah, GA, 2009, pp. 1943-1954.

[88] "XBee-PRO® 900/DigiMesh™ 900 RF Modules," Digi International Inc. 2009.

[89] K. C. Barr and K. Asanović, "Energy-aware lossless data compression," *ACM Trans. Comput. Syst.,* vol. 24, pp. 250-291, 2006.

[90] T. Schoellhammer, B. Greenstein, E. Osterweil, M. Wimbrow, and D. Estrin, "Lightweight temporal compression of microclimate datasets [wireless sensor networks]," in *Local Computer Networks, 2004. 29th Annual IEEE International Conference on*, 2004, pp. 516-524.